

Requirements of Efficient Deep Soil Mixing Treatment in Clayey Soils: A Field-based Assessment of Water Pre-drilling and Auger Free Blade Effects

Journal:	<i>Canadian Geotechnical Journal</i>
Manuscript ID	cgj-2024-0755.R3
Manuscript Type:	Research Article
Date Submitted by the Author:	28-Jun-2025
Complete List of Authors:	Alavi, Seyed Meisam; Iran University of Science and Technology, Civil Engineering; Baspar Pey Iranian, Soil improvement division Aghamolaei, Milad; Iran University of Science and Technology, Civil Engineering; Baspar Pey Iranian, Soil Improvement Division Shakeri Talarposhti, Sajjad; Iran University of Science and Technology, Civil Engineering; Baspar pey Iranian Khodaei Ardabili, Ahmad Ali; KN Toosi, Civil Engineering; Basparpey Iranian Company, Soil Improvement Division
Is the manuscript for consideration in a Special Issue or Collection?:	Not applicable (regular submission)
Keyword:	Deep soil mixing (DSM), Field investigation, Water pre-drilling phase, Auger free blade, Entrained mixing phenomenon

SCHOLARONE™
Manuscripts

Requirements of Efficient Deep Soil Mixing Treatment in Clayey Soils: A Field-based Assessment of Water Pre-drilling and Auger Free Blade Effects

Seyed Meisam Alavi ^{a*}

^{a*} *Corresponding Author*: Ph.D. of Geotechnical Engineering, School of Civil Engineering, Iran University of Science and Technology, Narmak, Tehran, Iran. Email: sm_alavi@civileng.iust.ac.ir

Milad Aghamolaei ^b

^b Ph.D. of Geotechnical Engineering, School of Civil Engineering, Iran University of Science and Technology, Narmak, Tehran, Iran. Email: m_ghamolaei@civileng.iust.ac.ir

Sajjad Shakeri Talarposhti ^c

^c Ph.D. of Geotechnical Engineering, School of Civil Engineering, Iran University of Science and Technology, Narmak, Tehran, Iran. Email: s_shakeri@civileng.iust.ac.ir

Ahmad Ali Khodaei Ardabili ^d

^d Ph.D. of Geotechnical Engineering, School of Civil Engineering, K.N. Toosi University of Technology, Tehran, Iran. Email: khodaie@dena.kntu.ac.ir

Abstract

Achieving a uniform/high-strength deep soil mixed (DSM) column and avoiding sticking cohesive soils to blades (i.e., entrained mixing/rotation phenomenon) requires multi-disciplinary involvement, including drilling tools configuration and mix designs. A series of 80 cm diameter DSM columns was executed in high cohesive clays using various drilling auger formations containing different numbers of free blades, and with/without water predrilling phases. Data interpretation was combined with full-depth coring and rig sensor records. The outcomes highlighted that adding free blades to the auger in a proper formation (dimensions/placement/shape/stiffness) resulted in uniform columns and facilitated the drilling by reducing the drilling pressure by about 40% while all the parameters were the same. The required

water discharge in the predrilling phase was formulated to aim for a water content (about 46%) beyond the liquid limit of clayey deposits (21-44%); a decisive technique to facilitate drilling in stiff cohesive soils. A 100% increase in the strength and a 50% enhancement in uniformity indexes in the executed columns of this project were achieved only through a tuned free-blade auger (number/configuration) and an optimal amount of added water. Besides, simultaneously implementing the predrilling phase and free blades to maximize drilling quality was inevitable due to their intertwined functions. Moreover, a new practical equation has also been proposed to consider the effect of free blades on the BRN within cohesive soil layers.

Keywords: Deep soil mixing (DSM), Field investigation, Mix design, Water pre-drilling phase, Auger free blade, Entrained mixing phenomenon.

1 Introduction

The construction above challenging soils has led to the need to carefully manage issues such as excessive ground settlements, soil-bearing capacity limitations, and the stabilization of the soil to ensure the safety of the structures using various soil improvement methods (Aghamolaei et al. 2025; Han 2015; Nicholson 2014). The Deep Soil Mixing (DSM) method is an advanced ground improvement technique that enhances soil properties by mixing chemical admixtures, such as cement, with in situ soils. The process of DSM results in improved strength and stability of the ground (Bruce et al. 2013; Han 2015). The DSM method's effectiveness in various soil types has made it a leading choice in numerous projects across various industries (Gupta and Kumar 2023; Topolnicki 2004, 2016). This method has been demonstrated to significantly enhance the

mechanical properties of expansive soils and address associated issues (e.g., Madhyannapu and Puppala (2014); Madhyannapu et al. (2009); Puppala et al. (2022)).

Investigations on structural properties, material composition, and manufacturing processes have uncovered numerous aspects (Alavi et al. 2024a; Nguyen et al. 2013; Shen et al. 2003; Yapage et al. 2014) and bring an invaluable asset for professionals and researchers (e.g., Lee et al. (2006), Boulanger and Idriss (2006); Ignat et al. (2016); Jiang et al. (2017); Jung et al. (2020); Liu et al. (2012); Yi et al. (2019); Yin and Fang (2010); Zhang et al. (2022); Zhang et al. (2019)).

Clayey soils cause significant challenges that can affect the quality of DSM columns. It is evident that there is a need for more thorough investigations that consider the practical implications and challenges of this condition which is limited in the literature. Chen et al. (2013) conducted a study on implementing the DSM method in soft clayey soil focusing on the sequence of DSM element installation and various construction parameters. Besides the soil condition, the volume of grouting, the water content of the soil-cement mixture, and the organic content play a crucial role in determining the overall quality of the mixing process (Filz et al. 2012). The impact of fines content within soil deposits on the strength of soil-cement specimens was examined by Teerawattanasuk and Voottipruex (2014). Moreover, Helson et al. (2017) explored the influence of varying clay content and binder factor levels on the unconfined compressive strength (UCS) of DSM columns.

As well as the soil condition, in practical aspects, drilling rigs and devices are also important in the quality of columns. The concepts and development process of DSM machines are addressed in previous research (Kirsch and Bell 2012; Terashi 2003). In the case of multiple-shaft drilling rigs, the augers usually rotate on different sides, and thus, this auger structure can automatically cut the stick-to-auger soil bulbs. In addition, multiple-shaft rigs have bracing plates

to keep the distance between multiple mixing shafts. These plates are also expected to prevent the entrained rotation phenomenon and cut the stuck soil bulbs (Kitazume 2013, 2024). In the case of coaxial double-layer shafts, the drilling tools consist of two coaxial shafts that can rotate on opposite sides of each other. Hence, in such systems, the possible generated stuck soil bulb by the rotation of the internal rod and mixing blades will be cut by the opposite rotation of the external mixing blades (GE et al. 2024).

The simple single-shaft drilling rigs are the most common DSM drilling devices, available with various power and torque capacities. The occurrence of the entrained mixing phenomenon (EMP) is limited only to drilling DSM columns in the cohesive clayey soil deposits, therefore, the original augers in the simple single-shaft rigs do not usually have free blades equipped on them in the first place. Hence, technical specifications need to be provided for adding free blades to single-shaft drilling tools. Moreover, integrating free blades to improve mixing quality in single shaft machines is discussed in previous studies, highlighting that the strength of the specimens will be enhanced with the use of free blades (Denies and Huybrechts 2015; Kirsch and Bell 2012; Kitazume 2013, 2024).

Kitazume and Terashi (2013) revealed that various construction parameters and the specific specifications of the drilling rig machine significantly affect the strength and quality of the soil-cement mixture. Some recent contributions consider incorporating cutting-edge machine learning algorithms, the mechanical features of drilling tools like augers and bits, and the implementation of data processing techniques. In part of a study by Esmaeili et al. (2014), the researchers delved into the comparative effectiveness of four-blade and six-blade augers in a laboratory-scale setting. Alavi et al. (2024c) performed a comprehensive field investigation to develop a highly efficient procedure for creating uniform and well-strengthened DSM columns. The study involved a

meticulous analysis of rig data, comprehensive large-scale field validation, and the implementation of a quality control and assurance program. The primary focus of the work was to identify an optimal mix design for highly cohesive soil deposits. With the machine learning prospect providing novel advancements, Alavi et al. (2024b) developed and implemented a sophisticated correlation algorithm to predict the relationship between Unconfined Compressive Strength (UCS) results and various drilling rig machine parameters.

A thorough survey of the existing literature indicates that, despite numerous contributions focused on the DSM method, significant uncertainties remain evident and require clear discussion. Prime examples are the configuration of drilling tools and the sufficiency of adding a predrilling phase. The auger is essential for effective soil mixing and cutting, and its design must be tailored to the specific soil type in various projects, which is not discussed in-depth and reveals a conspicuous gap in the available technical documents. Hence, the adequacy of incorporating a water predrilling phase into the implementation process of DSM columns while drilling in clayey soil deposits has been addressed in detail.

It can be acknowledged that while the concept of free blades was introduced earlier in the literature, there is currently a lack of quantitative data, practical advice, and information on the impact of the number of free blades, configurations, etc., in cohesive soil strata. Therefore, this study presents a comprehensive field investigation utilizing different auger types, varying in free-blade formation and location, to determine the optimal drilling auger configuration and quantitative information about them for drilling in cohesive soils. With the privileges of drilling machine data of over 580 DSM columns, full-depth continuous corings, and UCS tests, this study delves into the concept of the entrained mixing phenomenon (EMP), examines the pressure exerted on the rigs during drilling, and assesses the quality of soil-cement columns to evaluate the

effectiveness of different auger types in DSM applications within highly cohesive soil strata. The findings can bring favorable outcomes for professional engineers and scholars to use the gained experience in real projects for developing more sustainable infrastructures.

2 Project Description

The DSM soil improvement project is located in Hormozgan province, Iran. Hormozgan is located in the southern region of Iran, adjacent to the Persian Gulf. Its strategic location has led to the development of numerous industrial manufacturing projects. The project site encompasses approximately 40000 m² in a coastal area characterized by high water levels and challenging soil conditions, which may present risks to construction activities. To thoroughly assess the soil characteristics across various locations, a comprehensive soil investigation program has been implemented. This program includes in situ tests, such as standard penetration tests (SPTs), as well as laboratory analyses, including undrained triaxial tests and direct shear tests, and etc. Based on 28 geotechnical exploration borings of 40 m depth and corresponding field and laboratory tests, sublayer soils consisted of about 1.5 m silty sand (i.e., SM, based on Unified Soil Classification System (USCS)) underlayered by medium stiff, stiff, and hard lean clayey soils (CL) with undrained cohesion of 0.3-0.6 kg/cm² to more than 1.5-2 kg/cm² values. Table 1 presents a detailed description of this project's cohesive and challengeable subsoil layers. The project was conducted utilizing a Soilmec SR95 drilling rig, which is capable of constructing DSM columns with large diameters and length reaching up to 33 meters. This equipment provides a maximum torque of approximately 351 kN/m.

As stated in the introduction section, drilling tools such as auger are important in the quality of mixing. Fig. 1 delineates the detailed description of the manufactured drilling auger in this project for executing 80 cm diameter DSM columns with two layers of free blades (named FB-2

hereafter). The FB-2 auger encompasses two mixing blade layers (i.e., without any auger bits), one main cutting blade layer, and bottom drilling bits as primary destruction forces. Fig. 1 delineates various dimensions of free blades and distances between blades. Besides, the details of critical sections of the auger are shown in Fig. 2. The majority of drilling bits in this auger consisted of flat teeth bits that are more suitable for drilling in clayey soils (Figs. 2b and 2c). Besides, eight nozzle spots were implemented in this auger, as illustrated in Fig. 2d.

When designing augers and free blades, it is essential to consider several key factors. Fig. 3 illustrates several significant types of damage that may be incurred by the free blades if appropriate considerations are not taken into account. The power of the machine imposes limitations on the weight and height of the auger and its blades, necessitating an understanding of the total height restrictions. Furthermore, it is crucial that the blade be sufficiently rigid to withstand soil pressure without compromising its structural integrity. For instance, vertical bending of free blades has occurred in Fig. 3a due to weak upper/lower stiffeners of the supports of free blades (results of excessive pressures tolerated by free blades) and low height of free blades. The insufficient height of the free blades before bending was 15 cm in Fig. 3a (this is a 1.6 m diameter auger), which was then increased to 20 cm after rehabilitation. The covering diameter of the free blade layers should be at least 10 cm more than other mixing/cutting blades to ensure not rotating the free blades and cutting stick-to-auger soils, as depicted in Fig. 3b. In this figure, an insufficient free blade layer diameter of 0.85 m (in a 0.8 m diameter auger) was modified to 0.9 m to ensure the proper function of free blades (i.e., free blades get stuck in the adjacent soils and do not rotate along with mixing blades). Nevertheless, careful attention must be given to the design of the free blade width to prevent excessive rotary pressure and soil adhesion. As is shown in Fig. 3c, out-of-plane distortion of free blades occurred due to the unnecessary extra length (offset of

about 20 cm) for a 1.6 m diameter auger, resulting of dealing with bigger confront soil mass (and more opposite forces).

Fig. 3d exhibits another critical location of free blades in an auger. Severe corrosion between free blade O-ring plates and upper/lower supports has occurred due to their relative displacement during the rotation of mixing blades and auger shaft (and not rotating free blades). Besides, implementing a long distance (e.g., 45 cm) between free blades and upper/lower mixing blades can defect the functionality of free blades in preventing the formation of adhesive soil bulbs around the blades. As depicted in Fig. 3e, the long distance between the free blade layer and the lower cutting blade (45 cm) resulted in the defective functionality of the free blade in the lower part. As a result, the optimization of augers is closely linked to specific soil conditions and the power of the machinery, both of which can vary significantly among different sites and contractors.

3 Results and Discussion

3.1 Effect of Using a Mix Design Without a Water Pre-drilling Phase

The used mix design of this project included a water pre-drilling phase for all DSM columns, denoted as the WWGG drilling method in Table 2 (WWGG stands for water drilling, water lifting, grout drilling, and grout lifting phases). Table 2 also reports the characteristics of a mix design without a pre-drilling phase as a part of a field validation program before the execution of main DSM columns (named GG in Table 2, which includes only grout drilling and grout lifting phases).

Adding a water pre-drilling phase in the mix design dealing with stiff clayey deposits aims to facilitate drilling by decreasing soil resistance and excessive adhesion to the mixing blades. To this end, the in-situ soil water content (ω) must be increased beyond its liquid limit (LL) during the pre-drilling phase. Considering this assumption, the mix design parameters in the pre-drilling phase can be calculated as follows:

$$\omega_{desired} = \frac{W_{w,soil} + W_{add}}{W_{soil}} = \frac{(\omega \cdot V \cdot \gamma_d) + W_{add}}{V \cdot \gamma_d} \quad (1)$$

which $\omega_{desired}$ is the desired water content of the soil at the end of predrilling phase, $W_{w,soil}$ is the water weight in the soil volume per meter length of the DSM column (kg/m), V is the volume of DSM column per meter (m^3/m), W_{add} is the weight of added water in the predrilling/lifting phases (kg/m^3), W_{soil} is the soil weight (kg/m), and γ_d is the dry unit weight of the soil (kg/m^3).

The W_{add} parameter can be theoretically calculated by the following equation:

$$W_{add} = \frac{Q_w}{DS_w \cdot V} + \frac{Q_w}{LS_w \cdot V} \quad (2)$$

in which the Q_w is the water discharge as denoted in Table 2 (in Lit/min), DS_w is the drilling speed at the water predrilling phase (m/min), and LS_w is the lifting speed at the water predrilling phase (m/min). The optimum mix design is the one that satisfies the desired water content with the lowest possible execution time. Hence, the DS_w parameter should be considered the maximum achievable predrilling speed controlled by the power of drilling rig. Therefore, an initial feasible value should be considered for the DS_w parameter based on results of a field validation program, and/or previous experiences of the contractor and engineering judgment. Moreover, the previous experiences of the contractor shows that LS_w parameter in the prelifting phase can be up to about three times of DS_w . Considering this assumption and solving the combination of Equations 1 and 2 for Q_w , results in:

$$Q_w = 0.75 \times (\omega_{desired} - \omega) \times V^2 \times \gamma_d \times DS_w \quad (3)$$

In this project: $Q_w =$

$$0.75 \times (0.46 - 0.2) \times 0.503^2 \times 1667 \times 1.2 = 99 \cong 100 \text{ Lit/min}$$

Hence, it is feasible to determine the water discharge in the mix design of the predrilling phase by using Equation 3. In the current project, considering the ω of about 20%, $\omega_{desired}$ of about 46%

(See Table 1), DS_w of about 1.2 m/min, V of 0.503 m³/m, and γ_d of about 1667 kg/m³ in Equation 3, the Q_w is equals to 100 Lit/min, as denoted in Table 2. The following results obtained by various approaches considering a predrilling phase in the mix design, and implementation of an auger with free blades.

3.1.1 Visual Assessment of Drilling Rod and Auger

The adherence of clayey clods to the rod presents a common challenge in DSM projects, particularly within cohesive soil layers. To effectively address this issue, it is essential to employ appropriate mixing techniques and utilize suitable tools, such as augers. The drilling rod condition at the end of mixing for GG-FB2 column, is presented in Fig. 4. Excessive adhesion of the surrounding soils to the drilling rod in the lifting phase (in addition to adhesion to the auger) might lift the part of executed DSM column in the previous phase. The diameter of the soil bulb encircling the rod, as indicated in Fig. 4, approximates the diameter of the DSM column (0.8 m), suggesting the displacement and elevation of most of the injected and mixed soil cement to the surface ground as spoil. It should be noted that the spoil refers to the excess mixtures extracted from surrounding the drilling rod, which may include soil, grout, or a mixture of soil-cement.

Three parameters are involved in the occurrence of adhesion soil to the rod, 1: cohesion of the soil, 2: defects in the mixing tools, and 3: an inappropriate mix design. The mixing tools utilized in this project comprise both the auger and the connecting rods. It is essential for the rods and augers to maintain coherence and adaptability. Certain drilling rigs, such as the one employed here, are designed to be heavy and powerful, allowing for the implementation of large-scale columns that enhance operational efficiency. The typical columns executed with this rig have a diameter of 1.6 meters. In this instance, the rods of the device are appropriately sized to accommodate this level of power. However, when smaller diameter columns need to be constructed using the same

device (such as DSM columns with 0.8 m diameter in this study), relying on the same rod may present challenges. For example, the blade length for a 0.8 m diameter column is only approximately 26.5 cm, which can limit the mixing efficiency. Hence, in the case of 2: *defects in the mixing tools* in this project, the diameter of the drilling shaft was about 27 cm, originally designed for drilling DSM columns with a diameter of 1.6 m. At the same time, a thinner rod could also be adequate for drilling columns with a 0.8 m diameter. This obligatory increase (due to project limitations) in the lateral surface of the drilling rod increased the prone area for adhesion of the soil to the shaft. However, this defect was solved in the design process of the drilling auger. As depicted in Fig. 1, a transition zone was implemented in the upper part of the auger to reduce the shaft diameter from 27 cm to 18 cm. This modification in the auger acts as a preventive action to minimize the possibility of soil adhesion to the auger and the consequent formation of EMP.

Salvatore et al. (2022) shed light on the fact that the plasticity of clays increases the tendency of the material to congest the rotating blades, reduce mixing efficiency, and remain clustered in lumps (i.e., EMP), disaffecting the mechanical behavior of the soil-cement elements. The EMP is related to the sticking of soil clumps to the drilling auger, preventing the proper function of mixing blades. In this scenario, the auger blades stick in a cohesive soil bulb and cannot mix the soil layers to disrupt their structure, causing the entire soil mass to rotate along with the blades. Moreover, the injected grout may escape to the ground surface through a path adjacent to the drill shaft (i.e., grout spoil).

In the DSM projects, the operator assistant tries to wash and clean the rod during the lifting phase as long as the stuck-to-rod soils are wet and loose, as shown in Fig. 5a. In this situation, these stuck-to-rod or stuck-to-auger soils might be dropped due to the induced water pressure, result in observing a clean appearance of the drilling rod and auger and no detection of the EMP.

Besides, these stuck soil bulbs may be dropped due to their weight during the uplift phase, as illustrated in Fig. 5b. Hence, the visual evaluation of drilling a DSM column should be monitored carefully by a quality control expert.

3.1.2 Quality Assessment Based on Full-depth Continuous Coring, UCS tests, and Drilling Machine Data with/without Predrilling

The pre-drilling phase is a common practical procedure in highly cohesive soil layers. To show the importance of that, the executed columns with/without predrilling were cored to assess the quality and control the required parameters. Fig. 6 shows the core boxes of the example column of GG-FB2 derived from a full-depth continuous coring apparatus (with a double tube core barrel) and its re-core samples (i.e., another full-depth continuous core on the opposite side of the primary core to reevaluate the column quality, as mentioned in FHWA). As was expected, the findings illustrated poorly mixed samples, particularly in Fig. 6a. Significantly, core boxes exhibited vacant positions, indicating that certain unimproved specimens were washed away during coring. Furthermore, unwashed samples contained numerous soil lumps, significantly impacting the UCS results by creating weak zones prone to fracturing during testing.

The pre-drilling phase is essential for enhancing the efficiency of the drilling process during the grouting phase. It effectively reduces the bond between cohesive particles, thereby improving the uniformity of the constructed DSM columns. Figure 7 presents a quantitative comparison of columns executed with and without the water pre-drilling phase, utilizing machine data and archived full-depth coring databases. Figs. 7a and 7b represent the uniformity assessment results of the GG-FB2 and two elements executed with the predrilling phase divided in 1.5 m core runs based on two indicators: core recovery (CR) and percent treatment (PT). The CR is calculated by dividing the total length of the recovered core (i.e., treated and untreated soil specimens derived

from continuous coring, excluding washed samples and empty positions in the core box) by the total core run length (e.g., 1.5 m in this project), while in the PT index only the mixed soil-cement samples divide to the total core run length (Bruce et al. 2013). The quantitative assessment in Figs. 7a and 7b confirmed that the GG-FB2, a DSM column with a GG mix design, failed to meet the uniformity acceptance criteria of this project (i.e., $CR \geq 80\%$ and $PT \geq 80\%$, based on FHWA recommendation).

The recovered core material percentage from the GG column is significantly lower than that of the two other columns that underwent a water pre-drilling phase. In contrast, the columns labeled WWGG demonstrated a completely uniform composition throughout their total length. The GG column, however, exhibited inadequate mixing over a distance of up to 4 meters, resulting in a treatment percentage of less than 50% and corresponding low strength due to substantial unmixed portions.

Regarding the strength criteria, the results of UCS tests should be more than the specified design strength in each core run in a column (e.g., 2 MPa in the current project). The results of the UCS tests presented in Fig. 7c for column GG-FB2 elaborate on this twisted evaluation of strength/uniformity. The zero UCS values in this graph demonstrate that there was no eligible sample for the UCS test in this core run, which is the direct impact of the uniformity of a core run on its strength while WWGG elements have an adequate strength more than designed value.

The data logger system implemented in the SR-95 drilling rig machine captures various drilling parameters per 10 cm during the execution of DSM columns. In this regard, Figs. 7d to 7g shows the various pressures induced in the drilling machine in the downward and upward grout injection phases. The pull-down (Fig. 7d) and hoist (i.e., lifting, Fig. 7e) pressures represent the required forces for moving the drilling auger down and pulling it up, respectively. In addition, the

rotary pressures (Figs. 7f and 7g) denote the forces resulting from blade rotation, which contribute to the direct dealing with the shear strength of soil and signify the level of mixing energy expended. Overall, the trend of uniformity and strength is further supported by rig data, which indicate a notable increase in downward forces and rotary pressures, with an increase of up to 45%. This observation suggests that the in-situ soils are resisting proper mixing with the injected grout, highlighting the importance of the pre-drilling phase in achieving optimal results. Another important observation of rig data is the uniform and consistent values of columns with a pre-drilling phase, while the GG columns fluctuate considerably. The consistent trends in the rig imply that all parts of the columns are mixed equally while permanent fluctuation is noticed in the inhomogeneous soil cement mixture.

Comparing the pulldown pressures of the 0.8 m GG-FB2 column with the results of a field validation program of a twice diameter (1.6 m) DSM project in clayey soils (Alavi et al. 2024c) illustrates high values (more than 70 bar) of pulldown pressures in the last meter in Fig. 6d. Besides, Alavi et al. (2024b) reported over 3780 data of various rotary pressures for conducting 1.6 m diameter DSM elements in clayey soils. Considering the range of the reported values in these 3780 data, rotary pressures of more than 150 bar in column GG-FB2 were higher than 75% of similar values (about 95 bar) in the mentioned database which can be attributed to the presence of free blades. The proper function of these blades depends on preventing the rotation of stick-to-auger clays, which causes considerable pressure on the drilling machine.

3.1.3 Assessing Core Improvement Rate (C_i index)

The literature has noted the challenges of interpreting the core strength data of soil-cement columns (Chen et al. 2016; Liu et al. 2017). Therefore, as the necessity of simultaneously assessing a DSM column's uniformity and strength quality was previously mentioned, the core improvement rate

(C_i) method was considered when evaluating various auger columns. The C_i method was initially introduced by Yoshitake et al. (2004) for assessing jet grouting columns and followingly developed by Alavi et al. (2024c) for evaluating DSM elements. The method comprises six Improvement Levels (ILs) for every 20 cm cored sample, from poor mixing to an ideal soil cement. IL 1 contains almost homogeneous specimens with no lumps, IL 2 considers slightly weaker samples with minor clayey or sandy lumps, IL 3 includes discontinuous chipped but well-mixed samples that cannot be selected for UCS tests, IL 4 covers poorly mixed specimens with lots of lumps, IL 5 samples are almost-soil with few improved fragments, and IL 6 represents only-soil specimens without any improved sections. Using the C_i approach, the considered strength of DSM columns ($q_{considered}$) is calculated based on a combination of uniformity conditions (i.e., ILs) and UCS tests as follows:

$$q_{considered} = 0.01 \left[(IL_1 + IL_2) \times UCS_{average} + (IL_3 \times UCS_{average} \times f_{reduction}) \right] \quad (4)$$

where $q_{considered}$ is the representative strength of the DSM column based on improvement levels of C_i method, IL_i presents the ratio of the number of i^{th} improvement level specimens (20 cm core parts) to the total cored specimens of the column (in percentage), and $f_{reduction}$ is the reduction factor of the strength of samples classified as IL 3 (assumed to be 0.5 based on the recommendation of Yoshitake et al. (2004)), and $UCS_{average}$ represents the average values of all UCS tests conducted on the column. As presented in Equation 4, only IL 1, IL 2, and IL 3 (with a reduction factor) samples are involved in considering a representative strength for a DSM column.

The results highlighting the achieved uniformity and strength are presented in Fig. 8. As indicated in the diagram, the proportion of well-mixed sections in the GG columns is approximately 50% lower than that observed in the WWGG columns. Furthermore, the adaptive strength measured is below 1.25 MPa at the highest level, demonstrating a 60% reduction

compared to the average of the two WWGG elements. These findings suggest that the use of free blades alone does not ensure the uniformity of soil-cement columns without implementing effective pre-drilling strategies.

3.2 Effect of the Number of Free Blade Layers

As discussed in the previous section, adding free blade layers to the drilling auger results in further resistance against the formation of EMP. The resulted pressures broke the connections of the lower free blade layer after the execution of 288 DSM elements. It is essential to highlight that the connection of the free blades to the main rod represents a critical component that requires careful and conservative design. These connections should facilitate smooth rotation of the free blades without any interference from the main rod. Furthermore, they must possess adequate rigidity to withstand the pressures exerted by highly cohesive soil layers, thus preventing potential breakage. In addition to some practical design aspects about free blades and their potential damage possibilities mentioned in section 2, regular inspections should be conducted daily, alongside consistent lubrication, to ensure optimal performance and maintenance of these connections.

Following the breakage of the free blade, the upper one was extracted from the auger for overhauling and preventing potential future failure in connections, making an auger with one free blade layer at the bottom. Overall, considering the maintenance process and component failure, 57 DSM columns were executed without free blades (Named FB-0), 237 columns were implemented with only one layer of free blades (Named FB-1) and 288 columns were executed with two free blades (Named FB-2). All other drilling parameters (i.e., mix design, tools, locations, geotechnical condition) were the same and the captured differences in the quality of these DSM columns can be attributed directly to the augers. In this regard, Table 2 presents detailed information on six example columns executed with these three auger types.

3.2.1 Visual Evaluation of Drilling Auger

Figs. 9 to 11 illustrates the auger condition at the end of execution of DSM columns with augers FB-0, FB-1, and FB-2, respectively. Despite using a water predrilling phase in all of these cases, severe adhesion of the adjacent soil to the drilling auger was observed while drilling with FB-0. As displayed in Fig. 9, such intense formation of EMP led to the entrapment of the mixing blades within a cohesive soil mass. Although adding one layer of free blades at the bottom in auger FB-1 prevented the formation of EMP in the lower zone, a complete formation of EMP continued in the upper parts of DSM columns, as depicted in Fig. 10. Hence, the functionality of the lower free blades was confirmed but remained inadequate for a proper function of all blades (i.e., no rotation of free blades along with free rotation of mixing blades without stuck soil bulbs). On the contrary, Fig. 11 demonstrates sharp contrasts between the auger condition using FB-2 with two layers of free blades, considering results in Figs. 8 and 9. All blades were in a free position due to using FB-2. In the absence of a free blade to detach the soil that adheres to the rod, the auger may become completely covered in soil. This condition impedes its functionality, preventing effective mixing during both downward and upward movements, reducing blade rotation number, PT, and resulting in an inhomogeneous soil-grout admixture.

3.2.2 Interpretation of Drilling Machine Data

Fig. 12 compares average values of rig data in WW phases (pre drilling stage with water only) for 57, 237, and 288 DSM columns executed with augers FB-0, FB-1, and FB-2, respectively. Significant increases in drilling and lifting rotary pressures were captured due to the proper function of the free blades of auger FB-2 in Figs. 12a and 12b. Up to 50 bar discrepancies were detected between the rotary pressures of DSM columns executed with or without two free blade augers, especially in the upper half of the columns. A comparison of augers FB-0 and FB-1

illustrated that adding one layer of free blades at the bottom could not considerably affect such pressures. This ineffective behavior of the bottom free blades in rotary pressures indicates that only one free blade layer cannot prevent the formation of EMP in such a long auger with a length of more than 2 m.

A direct recognition of the formation of EMP is feasible by assessing hoist pressures in Fig. 12d. Hoist pressure refers to the upward forces necessary to raise the augers, which encompass the weight of the augers, rods, and the overburden of soil and cements. In the event of EMP, the sensors will detect any additional hoist pressure, enabling engineers to monitor these changes effectively. As illustrated in Figure 12d, such occurrences may result in pressure readings that are up to 100% higher than standard levels with an apparent fluctuation. Severe increases in hoist pressures (up to 40 bar) are demonstrated in Fig. 12d for the auger FB-0 columns, along with sudden decreases in these pressures due to the dropping of the stick-to-auger soils at the bottom of the columns and change in the geotechnical layer. A moderate increase-and-relieve behavior was also observed in the FB-1 columns. On the contrary, a uniform hoist pressure for FB-2 columns demonstrated that free blades well prevented EMP. It is essential to note that despite the faster lifting speed of the auger FB-2 in Fig. 12c, which induces more hoist pressures to the rig, hoist pressures were under control by adding free blades.

3.2.3 Inspection of Continuous Coring and UCS Tests

Continuous full-depth coring was conducted on two example columns of each auger after 28 days of the execution. Figs. 13 to 15 show the core boxes of these six DSM columns (mentioned in Table 2). Significant differences were obvious in the quality of core boxes. The auger FB-0 boxes contained many unmixed specimens (which were punched with a marker tip for better visual detection in Fig. 11). Moreover, core washing occurred in more than 3 m of the C1-FB0 column,

making unfilled positions in core boxes. An improvement in core conditions was identified in the core boxes of auger FB-1. However, it predominantly involved samples with numerous lumps (Fig. 14). Following up the core conditions of auger FB-2 in Fig. 15, thoroughly satisfying specimens were detected.

To quantitatively inspect the effect of adding free blades to augers on the quality of the core boxes, Figs. 16a and 16b demonstrate the CR and PT of every 1.5 m core run of six representative columns. Due to the nature of the CR parameter that covers both mixed and unmixed cores in its equation, only one of the FB-0 columns failed to pass the uniformity criterion in Fig. 16a. However, better uniformity of the FB-2 columns was traceable even using the CR factor. In contrast, notable disparities were evident concerning the PT parameter in Fig. 16b. While the PT values were higher for the FB-1 columns than the FB-0 ones, only the FB-2 columns conformed to the acceptable uniformity criterion.

Fig. 16c reports the UCS results of these columns in each core run. It should be noted that a zero value was allocated to core runs that did not have proper samples (i.e., integrated homogeneous specimens, not chipped mass samples) for the UCS test. A decisive superiority of FB-2 columns was evident because all samples met 2 MPa strength (acceptance criterion in this project). Many lumps in FB-1 specimens resulted in the failure of about half of the core runs (i.e., no UCS samples or lower than 2 MPa specimens).

Fig. 17 delineates the quality assessment of example DSM columns based on the C_i approach, a simultaneously representative of uniformity and strength condition. The cumulative percentage of improvement levels presented in Fig. 15a demonstrated that over 85% of the length of auger FB-2 columns were well-mixed soil-cement samples (i.e., IL 1, IL 2, and IL 3), while this value was about 62% and 30% for FB-1 columns, and 27% and 10% for FB-0 ones. The effect of

such discrepancies in the uniformity of these columns is highlighted in the representative strength of DSM columns depicted in Fig. 15b (using Equation 1). Although there were samples in FB-0 columns even with more than 2 MPa UCS, less than 0.4 MPa strength should be attributed to these columns based on the C_i method. Implementing one free blade layer increased the $q_{considered}$ up to 0.73 and 1.45 MPa; an inadequate enhancement. Hence, only FB-2 columns met the required design strength, as shown in Fig. 15b. Conducting an engineering judgment based on the C_i approach was entirely in line with all other assessment methods examined in this study, including continuous corings, PT criterion, UCS results, and drilling data.

As denoted in the literature (e.g., (Alavi et al. 2024c; Bruce et al. 2013; Kitazume and Terashi 2013)), it is essential to mention that an excessive increase in in-situ water content by a water predrilling phase (before the grout phase) can significantly affect the strength of the DSM columns. In this project, the geotechnical survey indicated that the LL of underlayer soils varies between 21-44%, especially with deeper depths of 6.5 m, which are stiff (LL of 21-42%) and very-stiff-to-hard soils (LL of 34-44%), as reported in Table 1. The mass production phase is usually executed with only one optimum mix design after initial field evaluation (as illustrated in Table 2). In such cases, the selected mix design should be capable of acceptable drilling quality in the worst soil conditions, which are the soils with the maximum LL value in this case (44%). Hence, the design of the mix designs is based on an assumption that all underlayer soils are in the worst condition, which is indeed a conservative design approach. Considering this design approach will guarantee the integrity and uniformity criterion of the DSM columns by providing the required soil water content in a predrilling phase. However, this approach has consequences. More than required in-situ water before grout mixing decreases the strength of DSM columns. Therefore, the

design engineer should carefully consider the probable lower strength of DSM columns in such cases and define the acceptable strength while paying attention to this matter.

Such dependency of the strength of DSM columns on the in-situ water in soil before grout drilling is also detectable in the presented results. For example, in Figure 7 (or Figure 16), there is up to a 2-3 MPa difference in the UCS values of a DSM column in various depths. Since the mix design and the volume of injected cement remain consistent, this variation in UCS values can be exclusively attributed to the geotechnical conditions of the soil prior to the initiation of grout drilling. Consequently, the acceptable UCS value established for this project was set at 2 MPa, as illustrated in Figures 7, 16, and 17.

3.3 Deficiencies of Blade Rotation Number (BRN) Parameter

The FHWA has proposed the BRN parameter as a simplified index of the quality of treated soil (Bruce et al. 2013):

$$BRN = n_b \left(\frac{N_d}{V_d} + \frac{N_l}{V_l} \right) \quad (5)$$

in which, n_b is the total number of mixing and cutting blades (not free blades, e.g., six blades in this project), N_d and N_l are the rotational speed during drilling and lifting of the GG phase (revolutions/min), respectively, and V_d and V_l are drilling and lifting speed of the of GG phase (m/min), respectively. There are crucial concerns regarding relying on the BRN parameter in its current form to evaluate the drilling quality. Although all executed DSM columns with various augers had the same mix design and theoretically the same BRN number, significant contrasts have been observed between these columns. Most defects of the BRN parameter can be attributed to neglecting the efficiency of rotating blades when dealing with EMP in cohesive soils. Qualitatively, the formation of EMP is equal to the losing functionality of mixing and cutting

blades, and this flaw reduces the real BRN of the mixing. Another notable deficiency pertains to the lack of consideration for the impacts of adding a predrilling phase in the formulation of BRN. As reported in Table 2, the BRN of the GG mix design was about 1.33 times that of the WWGG mix design, while considerably weaker mixing quality was identified in this study. Hence, destroying the soil fabrics and reaching the soil liquid limit state can decrease the intensity of EMP and facilitate the GG drilling phase.

Based on experiences and observations, two modification coefficients can be implemented in the BRN equation in cohesive soils to consider: I) the effect of adding a water predrilling ($\alpha_{predrilling}$) and II) the effect of using free blades ($\alpha_{free-blades}$), as follows:

$$BRN_{modified} = \alpha_{predrilling} \cdot \alpha_{free-blades} \cdot \left[n_b \left(\frac{N_d}{V_d} + \frac{N_l}{V_l} \right) \right] \quad (6)$$

As discussed before, the major contribution of adding a predrilling phase is related to increasing the primary soil water content (ω) to the LL value. The closer the ω to the LL , the more efficient the drilling quality in the grout mixing phase. Hence, the $\frac{\omega_{in-situ}}{LL}$ has been considered as the $\alpha_{predrilling}$ coefficient in Equation 6, in which $\omega_{in-situ}$ is the in-situ soil water content before the grout drilling phase that might have been increased to the LL by using a water predrilling phase. Furthermore, a maximum value of 1 should be considered for the $\alpha_{predrilling}$ parameter (in cases with $\omega_{in-situ}$ more than LL).

In the case of considering the effect of using free blades, the functionality area of each free blade layer should be considered first, as illustrated in Fig. 18. As depicted in this figure, there are n_b mixing zones for each drilling auger, and all free blades can only improve the drilling quality (by preventing the formation of EMP) in the $(n_b - 2)$ zones. The maximum number of free blade layers ($n_{f-layer}$) in an ideal drilling condition is equal to the $(\frac{n_b}{2} - 1)$, and each free blade layer

only affects two mixing zones. The absence of free blades in each layer and corresponding mixing zones in such cohesive soils means that the rotation of the mixing blades is entrained into a massive soil bulb and thus has no effect in increasing the BRN. Hence the $\alpha_{free-blades}$ can be calculated as:

$$\alpha_{free-blades} = \frac{2 + (\text{mixing zones affected by free blades})}{\text{Total mixing zones}} = \frac{2 + (2n_{f-layer})}{n_b} = \frac{1 + n_{f-layer}}{0.5 n_b} \quad (7)$$

Hence, the modified BRN equation is equal to:

$$BRN_{modified} = \frac{\omega_{in-situ}}{LL} \cdot \frac{1 + n_{f-layer}}{0.5 n_b} \cdot \left[n_b \left(\frac{N_d}{V_d} + \frac{N_l}{V_l} \right) \right] \quad (8)$$

Using the aforementioned equations, Table 3 represents the $BRN_{modified}$ parameter for seven example DSM columns presented in this study. Moreover, to quantitatively assess the $BRN_{modified}$ equation, Fig. 19 compares $BRN_{modified}$ of these columns with their uniformity/strength quality indexes, encompassing Total Percent Treatment (TPT, average of the PT parameter in all core runs), Total Core Recovery (TCR, average of the CR parameter in all core runs), and the $q_{considered}$ parameter (based on the C_i index). It should be noted that both the GG-FB2 column and its recore results are included in these graphs. As depicted in Fig. 19, fine correlations have been demonstrated between the proposed $BRN_{modified}$ and the TCR, TPT, and $q_{considered}$ parameters and quantitative comparisons and contrasts between columns are now feasible using this equation. The major contribution of such graphs in Fig. 19 can be dedicated to developing them for the field validation stage of DSM projects. For instance, the acceptance criteria in this study necessitate mix designs with $BRN_{modified}$ values more than 150 to satisfy 80% core recovery index (Fig. 19a), more than about 360 (the same as minimum acceptable BRN in FHWA) to meet the 80% percent treatment criterion (Fig. 19b), and more than 400 to achieve the required strength of 2 MPa (Fig. 19c, all columns have the same binder factor of 400 kg/m³).

4 Conclusion

An extensive field investigation was conducted in a cohesive clayey soil layer to clarify the efficiency of two drilling approaches: implementing a water predrilling phase and utilizing varying numbers of free blades in the drilling auger, concerning the quality of DSM columns. The results were concluded based on drilling rig data, uniformity, UCS, and visual factors discussed in this section. The most significant outcomes of the conducted field columns are as follows:

- The findings emphasize the critical need for meticulous execution programs. Adjusting the in-situ water content (about 46%) beyond the soil's liquid limit (21-44%) using a water predrilling phase effectively enhanced the strength/uniformity of DSM columns, along with decreasing drilling rig pressures. Simultaneous implementation of the water predrilling phase and adding free blades is imperative for projects with similar soil conditions to avoid the negative consequences of poorly mixed columns. Utilizing free blades without executing a water predrilling phase has yielded unfavourable outcomes. 100% increase in strength and mixing quality is achieved, it is essential to implement an appropriate and effective mixing method.
- The proper positioning of free blades is critical in mitigating the adhesion of the surrounding soils to the rods during the mixing process. Free blades must be correctly distributed across the entire auger length to effectively remove stuck soils from the rod. A long distance (e.g., 45 cm) between the free blades and upper/lower mixing blades can affect the proper functionality of the free blades (i.e., cutting the stick-to-auger soils). Besides, to ensure correct performance (i.e., no rotation of free blades along with free rotation of mixing blades), the free blade must be at least 10 cm larger than the cutting blade. This size difference is essential for the independent functionality of free blades.

- Based on extensive experience, it is recommended that a height of 10 and 20 cm are practical for free blades in 0.8 and 1.6 m diameter augers, respectively. The material selected for these blades should be both durable and reinforced with a stiffener for enhanced performance. Furthermore, the connection between the free blades and the rods should be designed with a conservative approach and monitored regularly from a maintenance perspective.
- Thorough consideration of using free blades and predrilling phases substantially increases the strength of specimens by at least 100% and the uniformity of columns by at least 50%. Visual examination of core boxes indicates improved column mixing by implementing an appropriate mix design.
- In the current codes, such as FHWA, the criteria for UCS and uniformity of the columns are evaluated separately. However, it is advisable to consider combining the results for a more comprehensive assessment. Using the core improvement rate (C_i index) for this purpose allows for a more thorough discussion of the best design scheme.
- Profound precautions should be taken when considering the BRN parameter as the representative factor of drilling quality. A new practical equation has been proposed that takes into account the effect of free blades on the BRN within cohesive soil layers. This development aims to enhance the accuracy and applicability of assessments in relevant engineering applications.

Acknowledgements

This study was carried out in collaboration with the Baspar Pey Iranian (BPI) Company. The authors sincerely appreciate this company for all the support.

Competing interests

The authors declare there are no competing interests.

Data availability statement

Data generated or analyzed during this study are available from the corresponding author upon reasonable request.

Draft

References

- Aghamolaei, M., Alavi, S.M., Shakeri Talarposhti, S., and Khodaei Ardabili, A.A. 2025. Assessing Jet Grouting Column Diameter in Loose to Medium Silty Soils Based on Field Observations. *Int. J. Geomech.*, (in press). doi: <https://doi.org/10.1061/IJGNAI/GMENG-11251>.
- Alavi, S.M., Aghamolaei, M., Khodaei Ardabili, A.A., and Shakeri Talarposhti, S. 2024a. Comprehensive Field Investigation on Effects of Drilling Auger Type on Quality of DSM Elements in Clayey Soils. *In Geo-Structures 2024*. pp. 120-133. doi: <https://doi.org/10.1061/9780784485842.012>.
- Alavi, S.M., Shakeri Talarposhti, S., Khodaei Ardabili, A.A., and Aghamolaei, M. Field Study on Unconfined Compressive Strength and Drilling Data of DSM Columns: A Machine Learning Approach. *In International Conference on Transportation and Development 2024*. 2024b. pp. 404-416. doi: <https://doi.org/10.1061/9780784485514.036>.
- Alavi, S.M., Aghamolaei, M., Shakeri Talarposhti, S., Khodaei Ardabili, A.A., and Salemi, S. 2024c. Efficiency Evaluation of Deep Soil Mixing Method in Stiff Clayey Soils: A Comprehensive Field Study. *Int. J. Geomech.* doi: <https://doi.org/10.1061/IJGNAI.GMENG-9893>.
- Boulanger, R.W., and Idriss, I.M. 2006. Liquefaction Susceptibility Criteria for Silts and Clays. *J. Geotech. Geoenviron. Eng.*, **132**(11): 1413-1426. doi: [https://doi.org/10.1061/\(ASCE\)1090-0241\(2006\)132:11\(1413\)](https://doi.org/10.1061/(ASCE)1090-0241(2006)132:11(1413)).
- Bruce, M.E.C., Berg, R.R., Filz, G.M., Terashi, M., Yang, D.S., Collin, J.G., and Geotechnica, S. 2013. Federal Highway Administration design manual: Deep mixing for embankment and

- foundation support. United States. Federal Highway Administration. Offices of Research & Development.
- Chen, E., Liu, Y., and Lee, F.-H. 2016. A statistical model for the unconfined compressive strength of deep-mixed columns **66**(5): 351-365. doi: <https://doi.org/10.1680/jgeot.14.P.162>.
- Chen, J.-J., Zhang, L., Zhang, J.-F., Zhu, Y.-F., and Wang, J.-H. 2013. Field tests, modification, and application of deep soil mixing method in soft clay. *J. Geotech. Geoenviron.*, **139**(1): 24-34. doi: [https://doi.org/10.1061/\(ASCE\)GT.1943-5606.0000746](https://doi.org/10.1061/(ASCE)GT.1943-5606.0000746).
- Denies, N., and Huybrechts, N. 2015. Deep mixing method: Equipment and field of applications. *In* Ground improvement case histories. Elsevier. pp. 311-350. doi: <https://doi.org/10.1016/B978-0-08-100191-2.00011-3>.
- Esmaili, M., Gharouni-Nik, M., and Khajehei, H. 2014. Evaluation of deep soil mixing efficiency in stabilizing loose sandy soils using laboratory tests **37**(5): 817-827. doi: <https://doi.org/10.1520/GTJ20130099>.
- Filz, G., Adams, T., Navin, M., and Templeton, A. 2012. Design of deep mixing for support of levees and floodwalls. *In* Grouting and Deep Mixing 2012. pp. 89-133. doi: <https://doi.org/10.1061/9780784412350.0004>.
- GE, C.-w., LIU, Z., YU, T.-x., LAN, W., YANG, N.-y., and ZHAO, M.-y. 2024. Model test study of key factors of deep soil mixing mechanism using contra-rotational shear method. *Rock and Soil Mech.*, **45**(1): 4. doi: <https://rocksoilmech.researchcommons.org/journal/vol45/iss1/4/10.16285/j.rsm.2023.5072>.

- Gupta, S., and Kumar, S. 2023. A state-of-the-art review of the deep soil mixing technique for ground improvement. *Innov. Infrastruct. Solut.*, **8**(4): 129. doi: <https://doi.org/10.1007/s41062-023-01098-6>.
- Han, J. 2015. Principles and practice of ground improvement. John Wiley & Sons. Available from <https://www.wiley.com/en-us/Principles+and+Practice+of+Ground+Improvement-p-9781118259917> [accessed].
- Helson, O., Beaucour, A.-L., Eslami, J., Noumowe, A., and Gotteland, P. 2017. Physical and mechanical properties of soilcrete mixtures: Soil clay content and formulation parameters. *Constr. Build. Mater.*, **131**: 775-783. doi: <https://doi.org/10.1016/j.conbuildmat.2016.11.021>.
- Ignat, R., Baker, S., Liedberg, S., and Larsson, S. 2016. Behavior of braced excavation supported by panels of deep mixing columns. *Can. Geotech. J.*, **53**(10): 1671-1687. doi: <https://doi.org/10.1139/cgj-2016-0137>.
- Jiang, Y., Zheng, G., and Han, J. 2017. Numerical Evaluation of Consolidation of Soft Foundations Improved by Sand–Deep-Mixed Composite Columns **17**(8): 04017034. doi: [https://doi.org/10.1061/\(ASCE\)GM.1943-5622.0000907](https://doi.org/10.1061/(ASCE)GM.1943-5622.0000907).
- Jung, C., Ceglarek, R., Clauvelin, T., Ayseldeen, M., and Kim, D. 2020. Deep soil mixing in Sabkha soils for foundation support in United Arab Emirates. *Int. J. Geosynth. Ground Eng.*, **6**(1): 3. doi: <https://doi.org/10.1007/s40891-020-0188-4>.
- Kirsch, K., and Bell, A. 2012. Ground improvement. CRC Press.
- Kitazume, M. 2013. Deep Mixing Method in Japan. *Geotechnical Engineering Journal of the SEAGS & AGSSEA*, **44**(4): 97-114. doi: <https://doi.org/10.14456/seagj.2013.11>.

- Kitazume, M. 2024. Deep mixing technology–diversity and future development. Japanese Geotechnical Society Special Publication, **11(2)**: 1-16. doi: <https://doi.org/10.3208/jgssp.vol11.KL-1>.
- Kitazume, M., and Terashi, M. 2013. The deep mixing method. CRC press. Available from <https://api.taylorfrancis.com/content/books/mono/download?identifierName=doi&identifierValue=10.1201/b13873&type=googlepdf> [accessed].
- Lee, F., Lee, C., and Dasari, G. 2006. Centrifuge modelling of wet deep mixing processes in soft clays **56(10)**: 677-691. doi: <https://doi.org/10.1680/geot.2006.56.10.677>.
- Liu, S.-Y., Du, Y.-J., Yi, Y.-L., and Puppala, A.J. 2012. Field investigations on performance of T-shaped deep mixed soil cement column–supported embankments over soft ground **138(6)**: 718-727. doi: [https://doi.org/10.1061/\(ASCE\)GT.1943-5606.0000625](https://doi.org/10.1061/(ASCE)GT.1943-5606.0000625).
- Liu, Y., Jiang, Y., Xiao, H., and Lee, F. 2017. Determination of representative strength of deep cement-mixed clay from core strength data. *Géotechnique*, **67(4)**: 350-364. doi: <https://doi.org/10.1680/jgeot.16.P.105>.
- Madhyannapu, R.S., and Puppala, A.J. 2014. Design and construction guidelines for deep soil mixing to stabilize expansive soils. *J. Geotech. Geoenviron. Eng.*, **140(9)**: 04014051. doi: [https://doi.org/10.1061/\(ASCE\)GT.1943-5606.0001149](https://doi.org/10.1061/(ASCE)GT.1943-5606.0001149).
- Madhyannapu, R.S., Puppala, A.J., Bhadriraju, V., and Nazarian, S. 2009. Deep Soil Mixing (DSM) treatment of expansive soils. *In Advances in Ground Improvement: Research to Practice in the United States and China*. pp. 130-139. doi: [https://doi.org/10.1061/41025\(338\)14](https://doi.org/10.1061/41025(338)14).

- Nguyen, T.V., Rayamajhi, D., Boulanger, R.W., Ashford, S.A., Lu, J., Elgamal, A., and Shao, L. 2013. Design of DSM Grids for Liquefaction Remediation. *J. Geotech. Geoenviron. Eng.*, **139**(11): 1923-1933. doi: [https://doi.org/10.1061/\(ASCE\)GT.1943-5606.0000921](https://doi.org/10.1061/(ASCE)GT.1943-5606.0000921).
- Nicholson, P.G. 2014. Soil improvement and ground modification methods. Butterworth-Heinemann.
- Puppala, A.J., Madhyannapu, R.S., and Nazarian, S. 2022. Full-scale field studies to evaluate deep soil mixing in stabilizing expansive soils. *J. Geotech. Geoenviron. Eng.*, **148**(1): 04021163. doi: [https://doi.org/10.1061/\(ASCE\)GT.1943-5606.0002647](https://doi.org/10.1061/(ASCE)GT.1943-5606.0002647).
- Salvatore, E., Modoni, G., Spagnoli, G., Arciero, M., Mascolo, M.C., and Ochmański, M. 2022. Conditioning clayey soils with a dispersant agent for Deep Soil Mixing application: laboratory experiments and artificial neural network interpretation **17**(11): 5073-5087. doi: <https://doi.org/10.1007/s11440-022-01505-9>.
- Shen, S.-L., Miura, N., and Koga, H. 2003. Interaction mechanism between deep mixing column and surrounding clay during installation. *Can. Geotech. J.*, **40**(2): 293-307. doi: <https://doi.org/10.1139/t02-109>.
- Teerawattanasuk, C., and Voottipruex, P. 2014. Influence of clay and silt proportions on cement-treated fine-grained soil **26**(3): 420-428. doi: [https://doi.org/10.1061/\(ASCE\)MT.1943-5533.0000813](https://doi.org/10.1061/(ASCE)MT.1943-5533.0000813).
- Terashi, M. 2003. The state of practice in deep mixing methods. *In Grouting and ground treatment*. pp. 25-49. doi: [https://doi.org/10.1061/40663\(2003\)2](https://doi.org/10.1061/40663(2003)2).
- Topolnicki, M. 2004. In situ soil mixing **2**: 331-428. Available from <https://www.taylorfrancis.com/chapters/edit/10.1201/b13678-13/situ-soil-mixing-micha%C5%82-topolnicki> [accessed].

- Topolnicki, M. General overview and advances in Deep Soil Mixing. *In XXIV geotechnical conference of torino design, construction and controls of soil improvement systems*. 2016. pp. 25-26.02.
- Yapage, N., Liyanapathirana, D., Kelly, R.B., Poulos, H.G., and Leo, C.J. 2014. Numerical modeling of an embankment over soft ground improved with deep cement mixed columns: case history. *J. Geotech. Geoenviron. Eng.*, **140**(11): 04014062. doi: [https://doi.org/10.1061/\(ASCE\)GT.1943-5606.0001165](https://doi.org/10.1061/(ASCE)GT.1943-5606.0001165).
- Yi, Y., Liu, S., Puppala, A.J., and Jing, F. 2019. Variable-diameter deep mixing column for multi-layered soft ground improvement: Laboratory modeling and field application **59**(3): 633-643. doi: <https://doi.org/10.1016/j.sandf.2019.01.009>.
- Yin, J.-H., and Fang, Z. 2010. Physical modeling of a footing on soft soil ground with deep cement mixed soil columns under vertical loading **28**(2): 173-188. doi: <https://doi.org/10.1080/10641191003780872>.
- Yoshitake, I., Nakagawa, K., Mitsui, T., Yoshikawa, T., and Ikeda, A. 2004. An evaluation method of ground improvement by jet grouting **19**(4-5): 496-497.
- Zhang, D., Wang, A., and Ding, X. 2022. Seismic response of pile groups improved with deep cement mixing columns in liquefiable sand: Shaking table tests. *Can. Geotech. J.*, **59**(6): 994-1006. doi: <https://doi.org/10.1139/cgj-2020-0505>.
- Zhang, Z., Ye, G., Cai, Y., and Zhang, Z. 2019. Centrifugal and numerical modeling of stiffened deep mixed column-supported embankment with slab over soft clay. *Can. Geotech. J.*, **56**(10): 1418-1432. doi: <https://doi.org/10.1139/cgj-2018-0180>.

Tables:**Table 1.** Characteristics of soil layers

Layer	Soil type (USCS)	Depth (m)	Strength classification	Moisture content (ω) (%)	Liquid limit (LL) (%)	Dry density (γ_d) (g/cm ³)	Friction angle (ϕ) (°)	Cohesion (c_u) (kg/cm ²)	Modulus of Elasticity (E) (kg/cm ²)	Poisson's ratio (ν)	Void ratio (e)	Over consolidation ratio (OCR)
S1	SM	0 – 1.5	Medium dense	5 - 10	-	1.65-1.75	31 - 33	0	200 - 300	0.33 – 0.35	-	-
S2	CL	1.5 – 6.5	Medium stiff	15 – 30	28 – 36	1.55-1.65	0	0.3 – 0.6	80 - 160	0.45 – 0.50	0.8 – 1.1	1 – 1.1
S3	CL	6.5 - 9	Stiff	10 - 25	21 - 42	1.65-1.75	0	1 – 1.5	270 - 400	0.40 – 0.45	0.6 – 0.7	1.1 – 1.5
S4	CL	9 - 40	Very stiff to hard	10 - 20	34 - 44	1.75-1.85	0	> 1.5 – 2	> 400 - 450	0.35 – 0.45	0.4 – 0.5	> 4

Table 2. Detailed description of DSM columns and corresponding mix design

Mix design type	Example column index	Auger condition	Column length - diameter	Drilling / Lifting grout volume	Grout discharge (Q)	Water discharge (Q_w)	Binder factor (a)	Water-to-binder ($w:b$)	Total water-to-binder ($w_t:b$) ^a	Predicted Blade Rotation Number (BRN) ^a	Grout drilling speed	Grout lifting speed	Water drilling speed	Water lifting speed	Expected time of an 8 m column
			m	%	Lit/min	Lit/min	Kg/m ³	-	-	1/m	m/min	m/min	m/min	m/min	min
GG	GG-FB2	FB-2 ^b	6.3 – 0.8	80 / 20	120	-	400	1	1.86	600	0.57	2.27	-	-	17.7
	C1-FB0	FB-0 ^c	12 – 0.8												
	C2-FB0	FB-0	8 – 0.8												
WWGG	C1-FB1	FB-1 ^d	8 – 0.8	90 / 10	150	100	400	0.8	2.07	450	0.74	Max (3.6)	1.2	Max (3.6)	21.9
	C2-FB1	FB-1	12 – 0.8												
	C1-FB2	FB-2	8 – 0.8												
	C2-FB2	FB-2	12 – 0.8												

^a Based on FHWA equations (Bruce et al. 2013)

^b Auger with two layers of free blades (as displayed in Fig. 1)

^c Auger without free blades

^d Auger with one layer of free blades (as displayed in Fig. 8)

Table 3. Values of $BRN_{modified}$ parameter for investigated DSM columns

Mix design type	Number of Free blade layers	Example column index	Average soil water content (ω) %	Average Liquid Limit (LL) %	Predicted in-situ water content before grout mixing phase ($\omega_{in-situ}$) %	$\alpha_{predrilling}$ ≤ 1	$\alpha_{free-blades}$ -	$BRN_{modified}$ -
GG	2	GG-FB2	20	44	20	0.45	1	270
	0	C1-FB0 & C2-FB0	20	44	46	1	0.33	148
WWGG	1	C1-FB1 & C2-FB1	20	44	46	1	0.67	301
	2	C1-FB2 & C2-FB2	20	44	46	1	1	450

Draft

List of Figures:

Fig. 1. Detailed descriptions of manufactured drilling auger of 80 cm diameter DSM columns with two free blade layers

Fig. 2. Details of drilling auger: a) free blade layer, b) using flat teeth bits at the bottom of the auger, c) simultaneously use of bullet and flat teeth bits for the cutting blades, and d) implemented nozzle spots

Fig. 3. Various possible damages of free blade layer: a) Vertical bending, b) Inadequate length of free blade layer, c) out-of-plane distortion, d) corrosion at connection between free blades and auger shaft, and e) long distance between free blade layer and mixing blades

Fig. 4. Excessive adhesion of adjacent soil to the drilling rod in a DSM column without a water predrilling phase

Fig. 5. Dropping of stuck-to-auger soil bulbs due to: a) water pressure during rod washing, b) weight of soil bulb phase

Fig. 6. Core box condition of a DSM column conducted without water predrilling phase and with auger FB-2

Fig. 7. Comparison of DSM columns with/without a water predrilling phase based on: a) core recovery), b) percent treatment, c) UCS, d) pulldown pressure of drilling auger, e) hoist pressure, f) rotary pressure at the drilling phase, and g) rotary pressure at the lifting phase

Fig. 8. a) Improvement levels of example DSM columns executed with/without a water predrilling phase (with the same number of free blades) various augers based on C_i evaluation method, and b) DSM column's representative strength based on C_i method and simultaneously considering uniformity and UCS results (based on Equation 4)

Fig. 9. Visual condition of auger FB-0 (without free blades) after drilling DSM columns

Fig. 10. a) Losing lower free blade layer due to high drilling pressures in stiff clayey soils, and b) visual condition of auger FB-1 (with one free blade layer) after drilling DSM columns

Fig. 11. Visual condition of auger FB-2 (with two free blade layers) after drilling DSM columns

Fig. 12. Average of drilling machine parameters for DSM columns executed with various augers in the WW phases: a) rotary pressure at the drilling phase, b) rotary pressure at the lifting phase, c) auger lifting speed, and d) auger hoist pressure

Fig. 13. Core box condition of DSM columns executed with auger FB-0 (without free blades)

Fig. 14. Core box condition of DSM columns executed with auger FB-1 (with one free blade layer)

Fig. 15. Core box condition of DSM columns executed with auger FB-2 (with two free blade layers)

Fig. 16. Characteristics of example DSM columns executed with various augers: a) uniformity criterion (core recovery), b) uniformity criterion (percent treatment), and c) strength criterion (UCS test results)

Fig. 17. a) Improvement levels of example DSM columns executed with various augers based on C_i evaluation method, and b) DSM column's representative strength based on C_i method

Fig. 18. Configuration of Mixing/Free blades and mixing zones in any desired auger with various blades

Fig. 19. Correlations between $BRN_{modified}$ parameter and quality indexes of DSM columns: a) core recovery, b) percent treatment, and c) representative strength based on C_i method

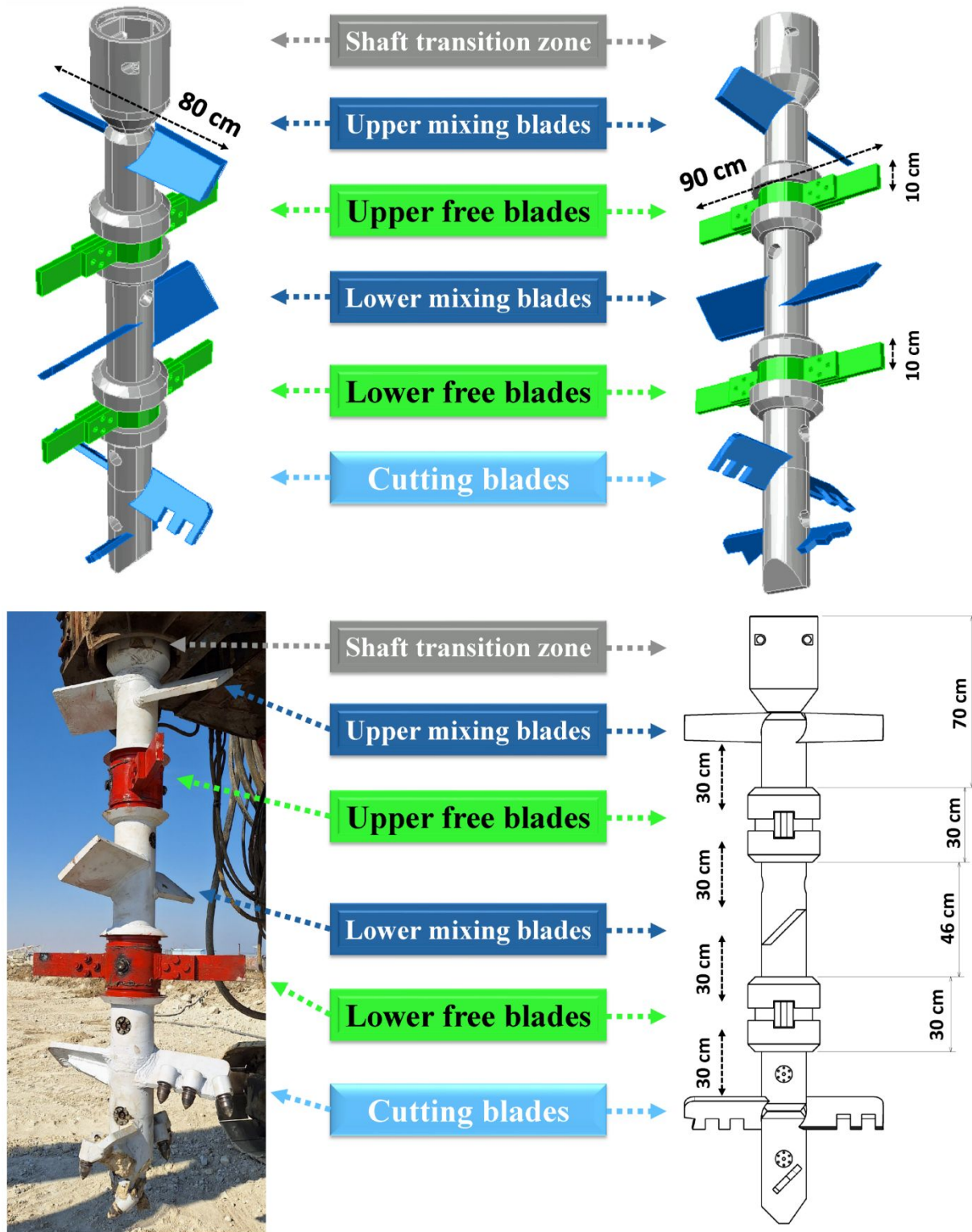


Fig. 1. Detailed descriptions of manufactured drilling auger of 80 cm diameter DSM columns with two free blade layers

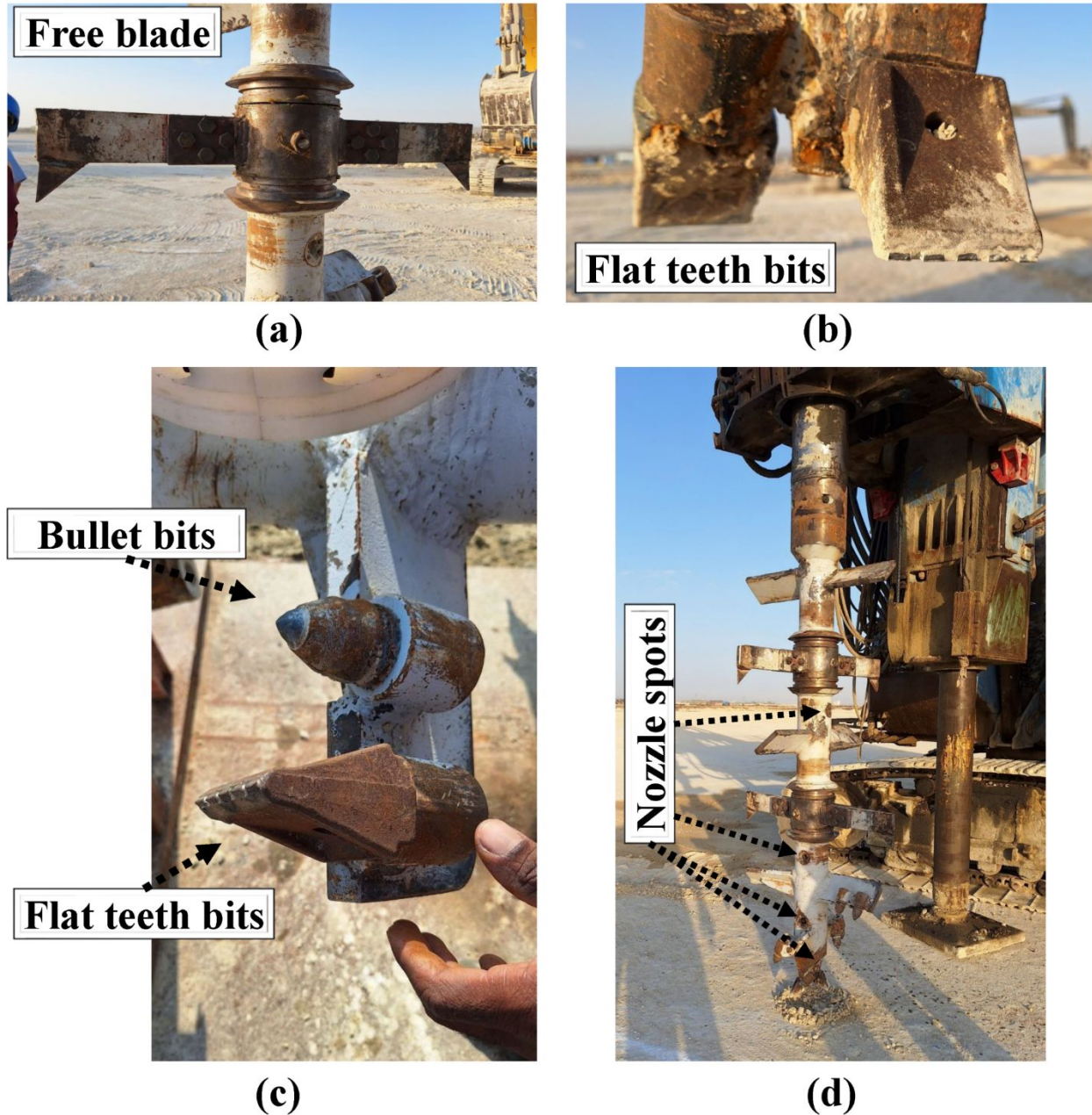


Fig. 2. Details of drilling auger: a) free blade layer, b) using flat teeth bits at the bottom of the auger, c) simultaneously use of bullet and flat teeth bits for the cutting blades, and d) implemented nozzle spots

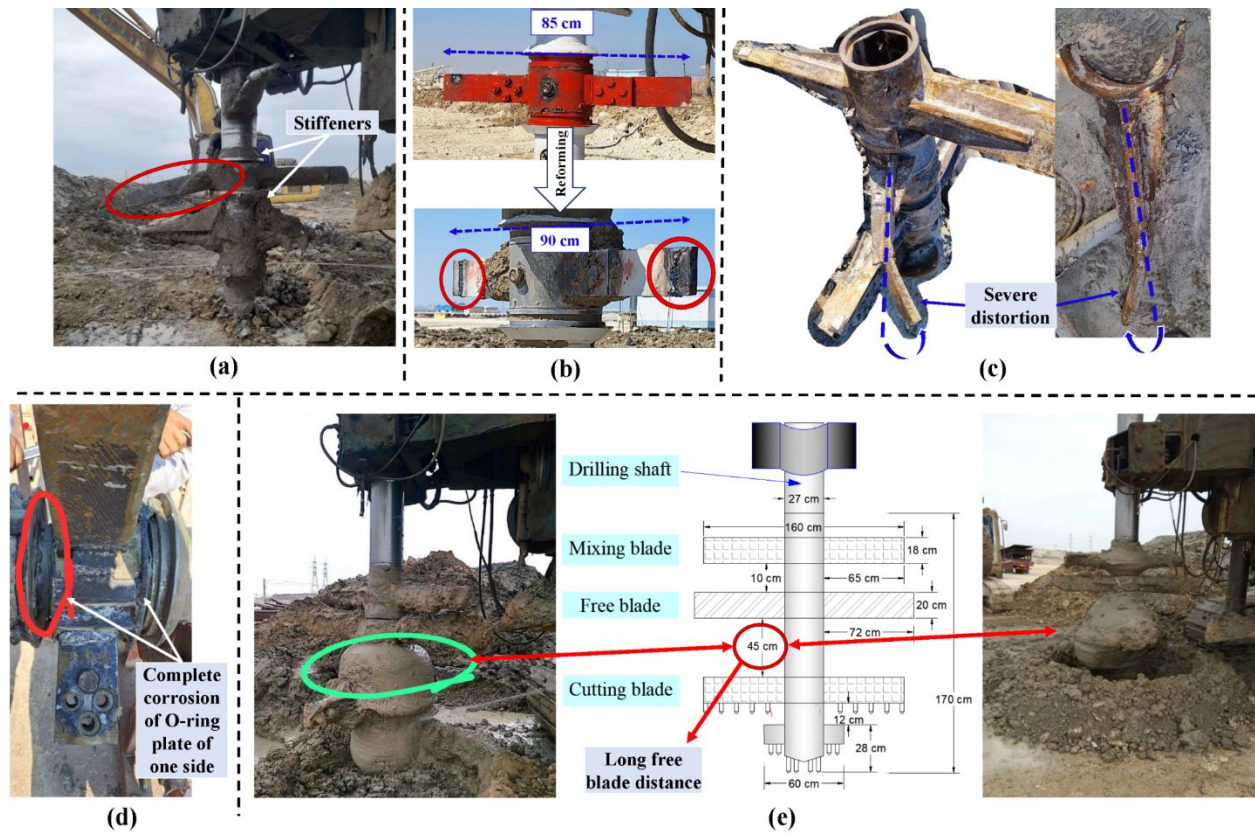


Fig. 3. Various possible damages of free blade layer: a) Vertical bending, b) Inadequate length of free blade layer, c) out-of-plane distortion, d) corrosion at connection between free blades and auger shaft, and e) long distance between free blade layer and mixing blades

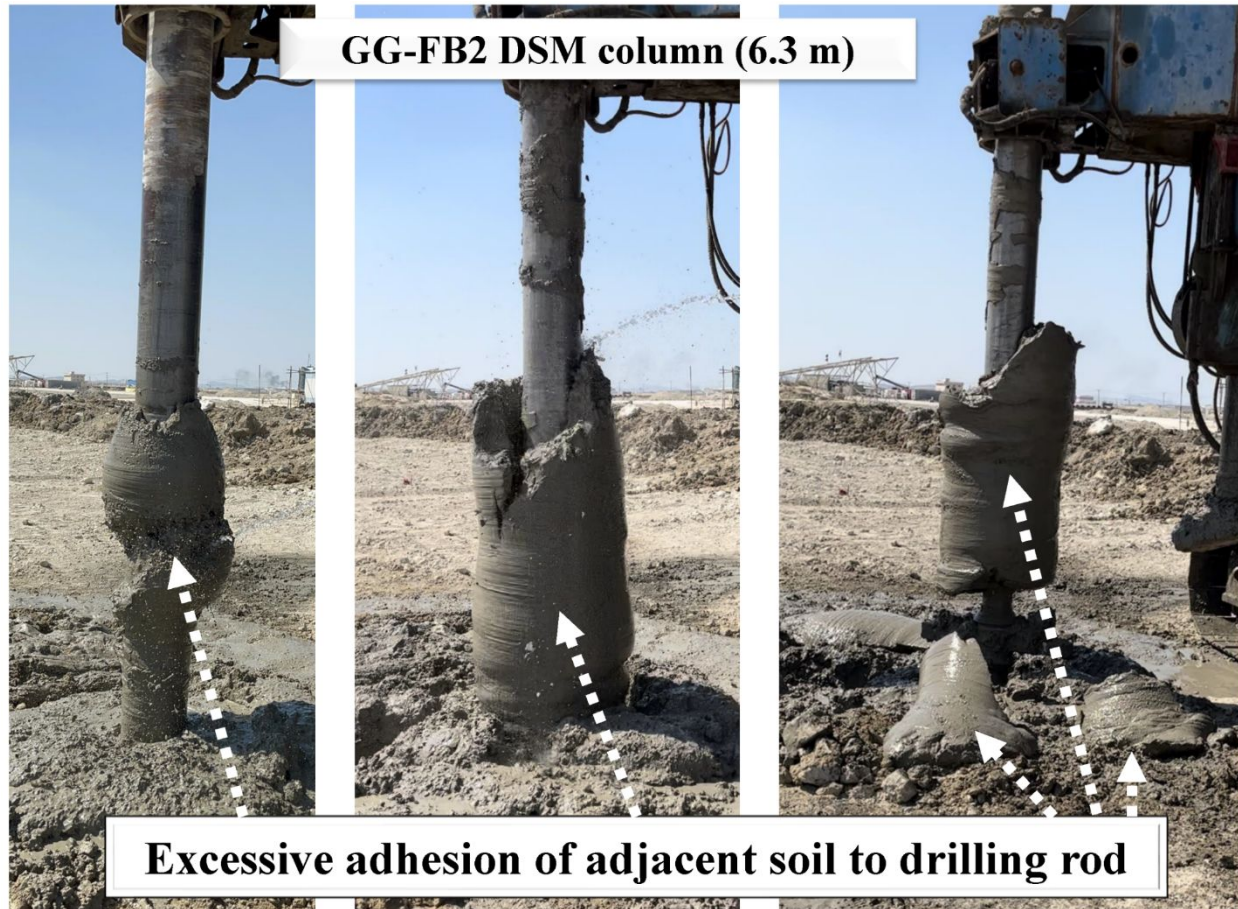


Fig. 4. Excessive adhesion of adjacent soil to the drilling rod in a DSM column without a water predrilling phase

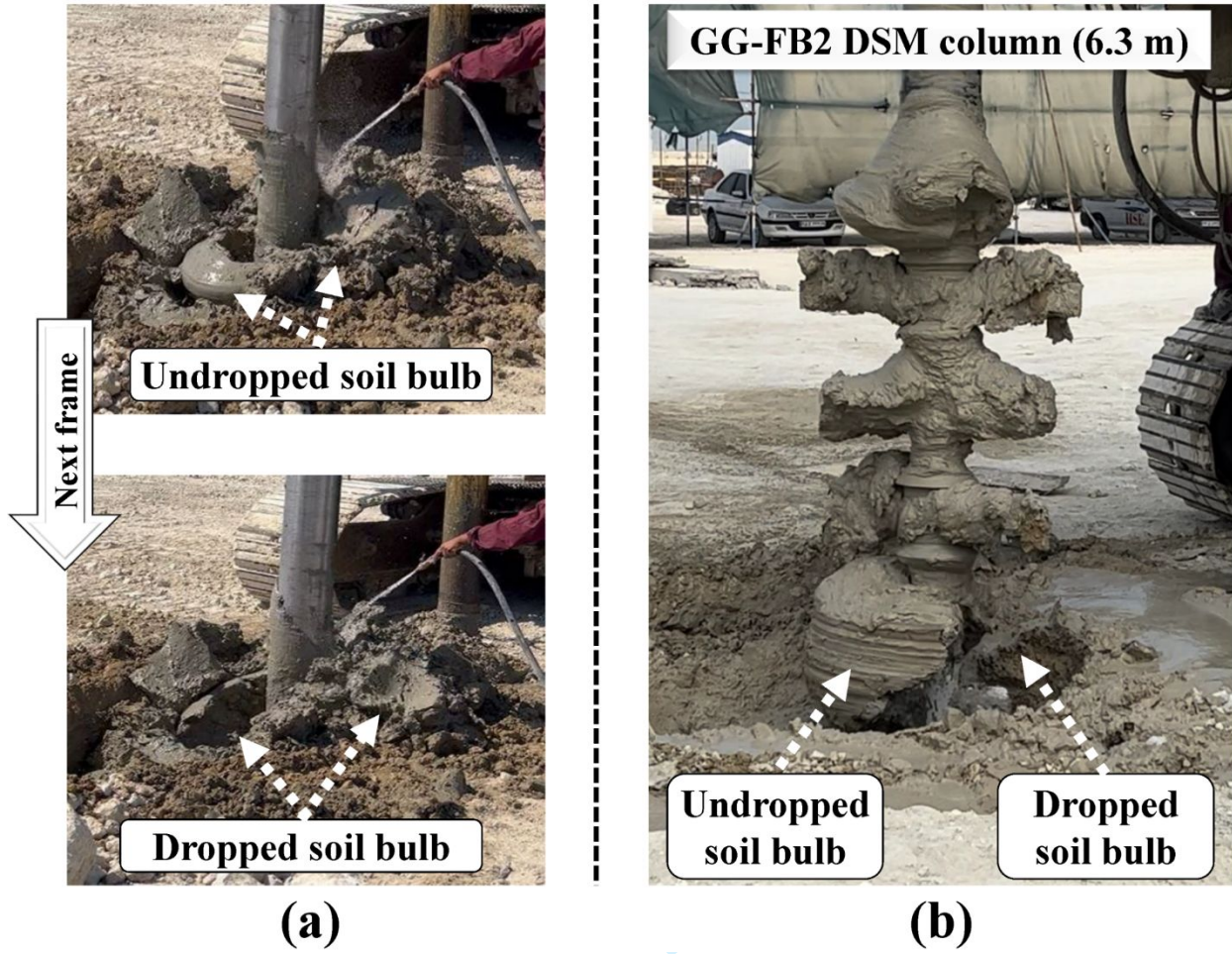


Fig. 5. Dropping of stuck-to-auger soil bulbs due to: a) water pressure during rod washing, b) weight of soil bulb phase

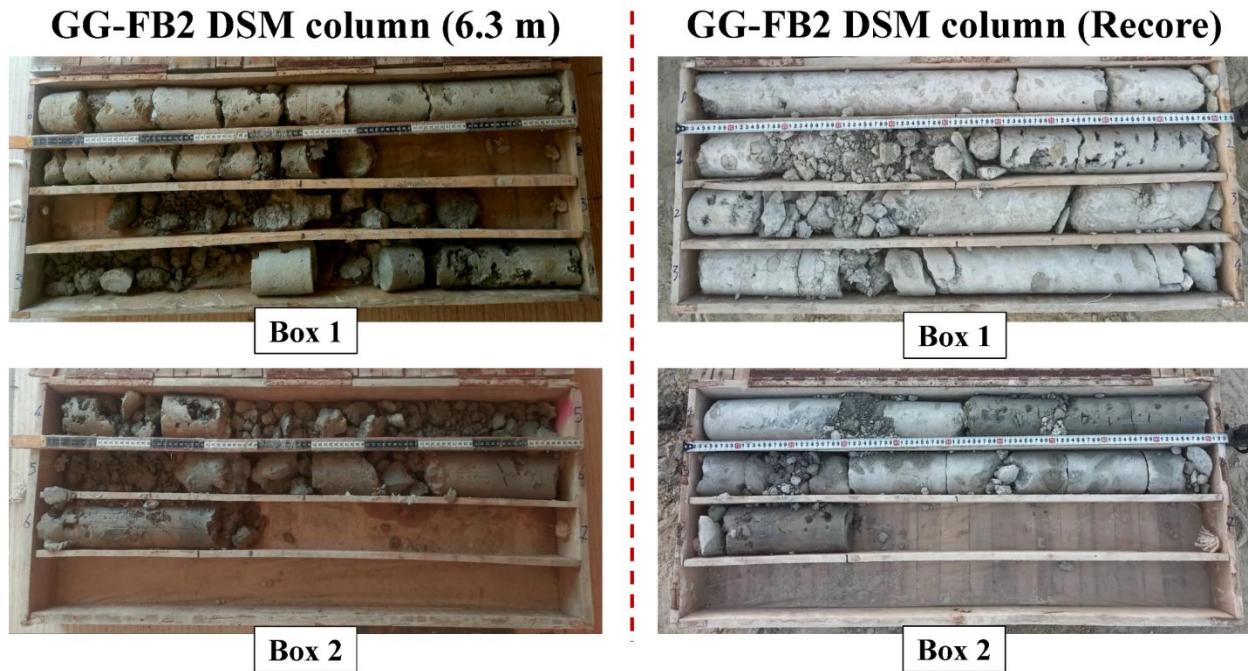


Fig. 6. Core box condition of a DSM column conducted without water predrilling phase and with auger FB-2

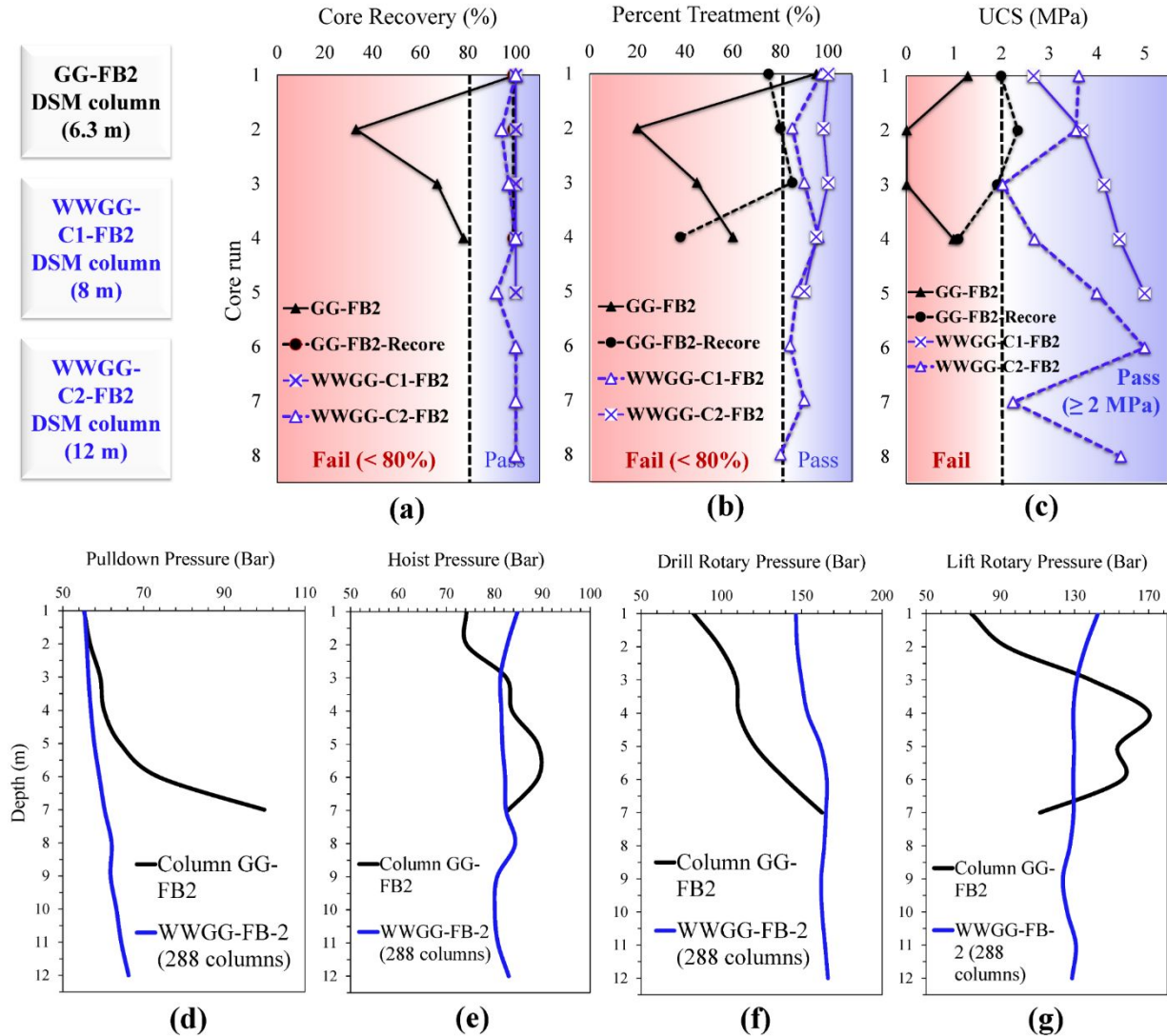


Fig. 7. Comparison of DSM columns with/without a water predrilling phase based on: a) core recovery), b) percent treatment, c) UCS, d) pull-down pressure of drilling auger, e) hoist pressure, f) rotary pressure at the drilling phase, and g) rotary pressure at the lifting phase

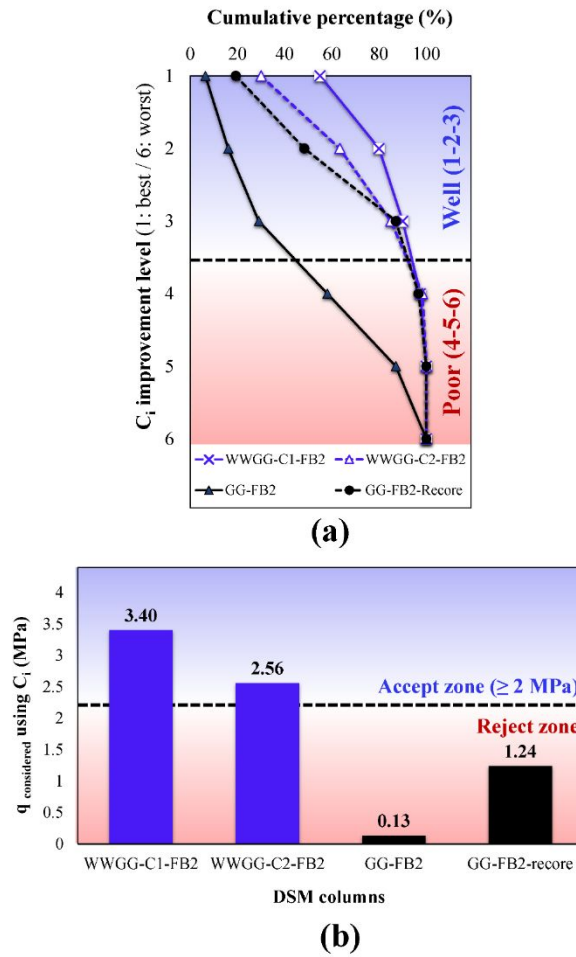


Fig. 8. a) Improvement levels of example DSM columns executed with/without a water predrilling phase (with the same number of free blades) various augers based on C_i evaluation method, and b) DSM column's representative strength based on C_i method and simultaneously considering uniformity and UCS results (based on Equation 4)



Fig. 9. Visual condition of auger FB-0 (without free blades) after drilling DSM columns

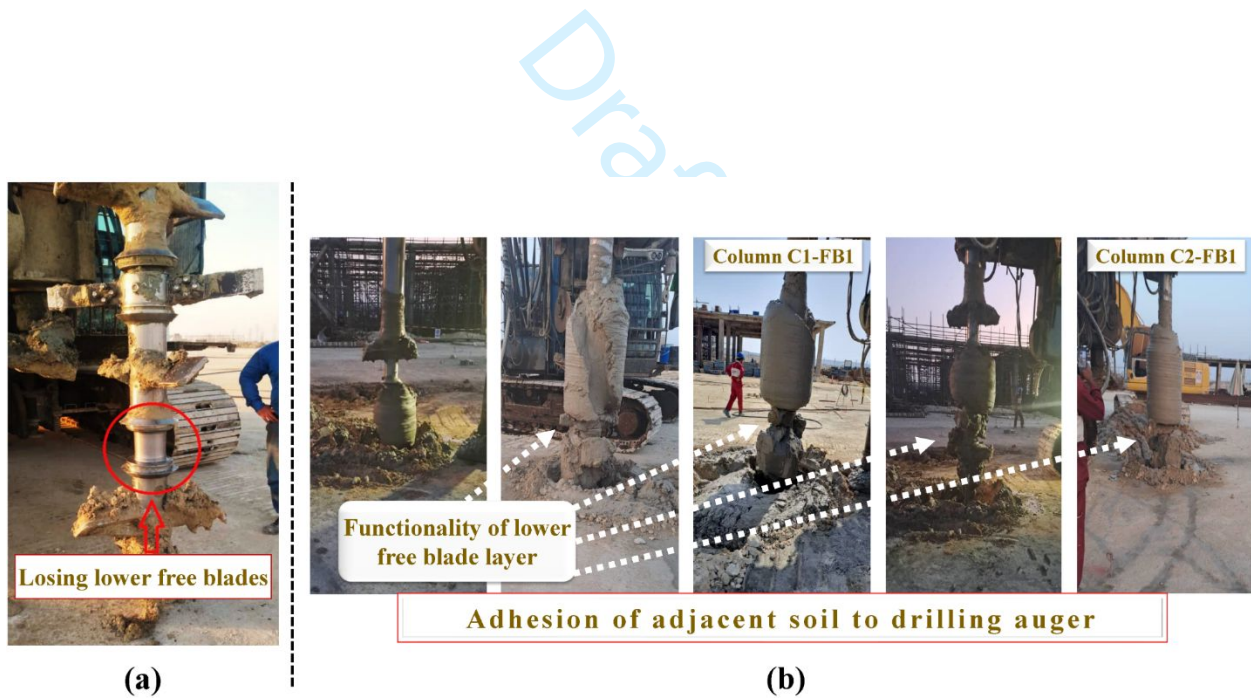


Fig. 10. a) Losing lower free blade layer due to high drilling pressures in stiff clayey soils, and b) visual condition of auger FB-1 (with one free blade layer) after drilling DSM columns

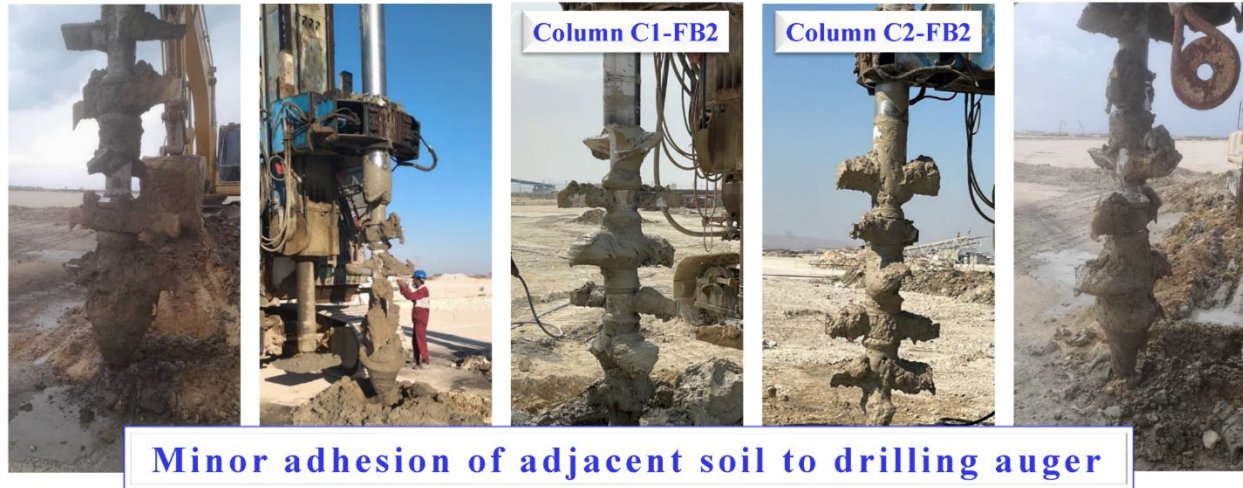


Fig. 11. Visual condition of auger FB-2 (with two free blade layers) after drilling DSM columns

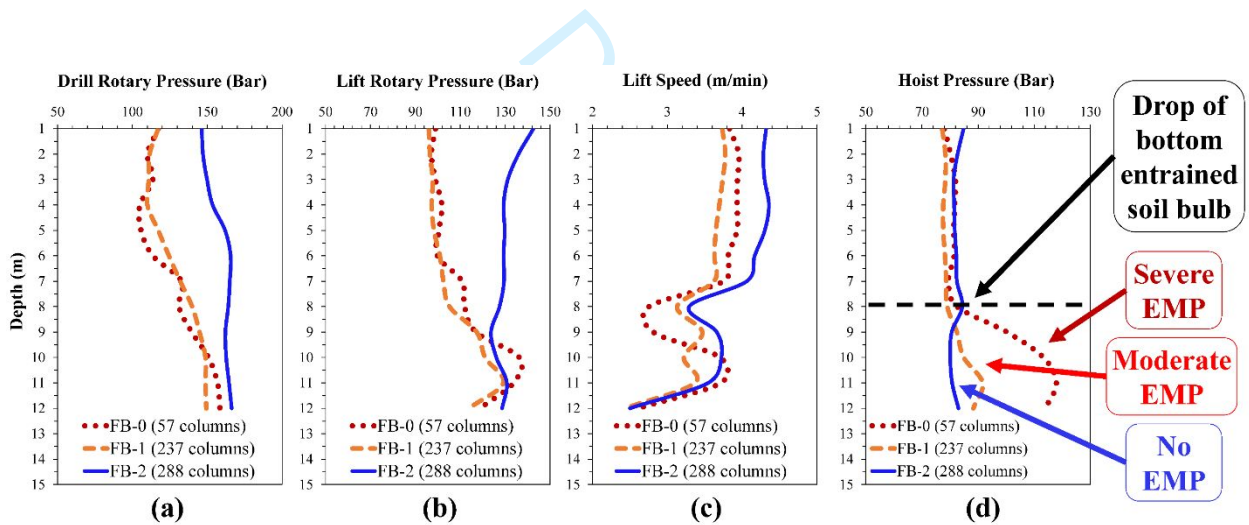


Fig. 12. Average of drilling machine parameters for DSM columns executed with various augers in the WW phases: a) rotary pressure at the drilling phase, b) rotary pressure at the lifting phase, c) auger lifting speed, and d) auger hoist pressure

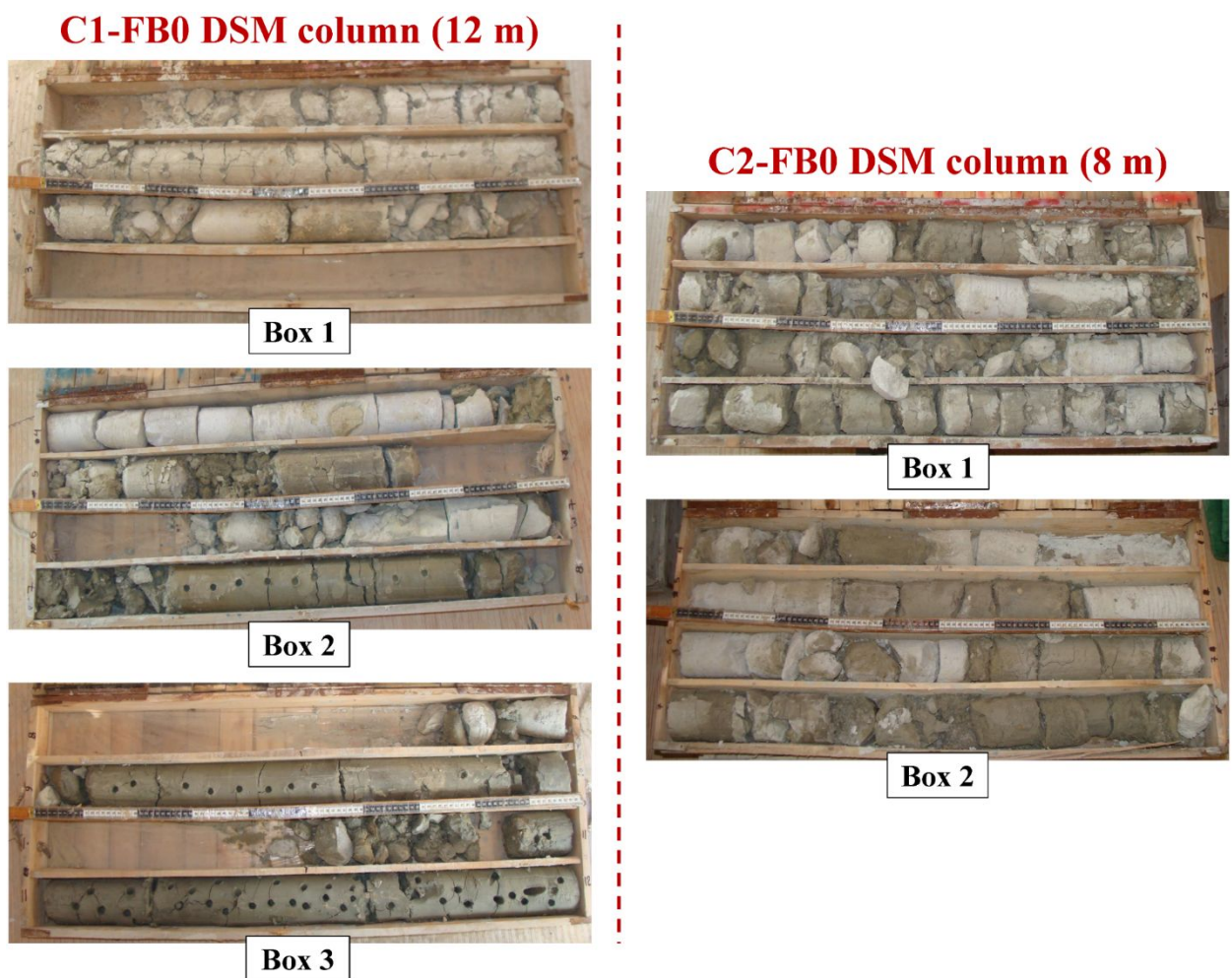


Fig. 13. Core box condition of DSM columns executed with auger FB-0 (without free blades)

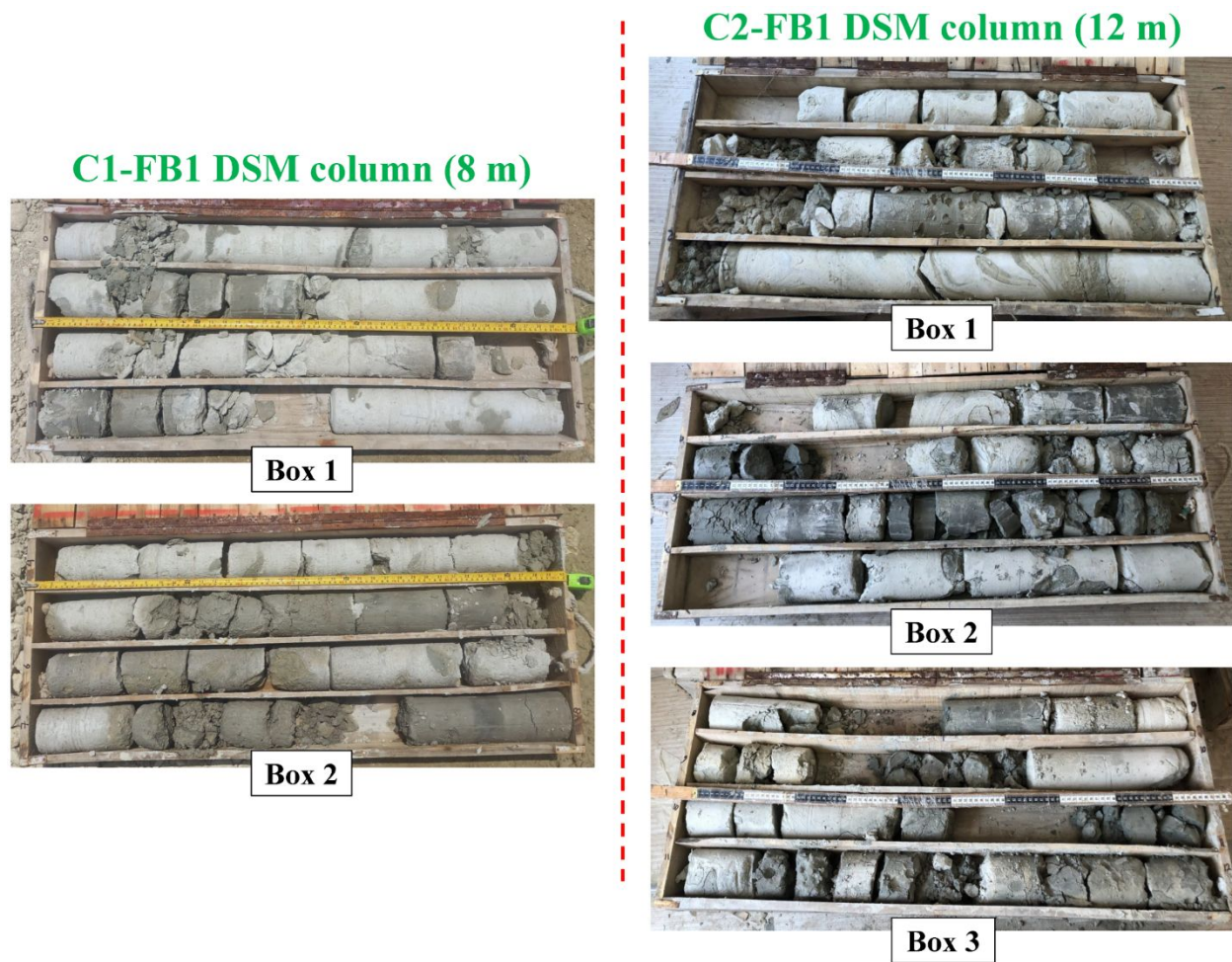


Fig. 14. Core box condition of DSM columns executed with auger FB-1 (with one free blade layer)

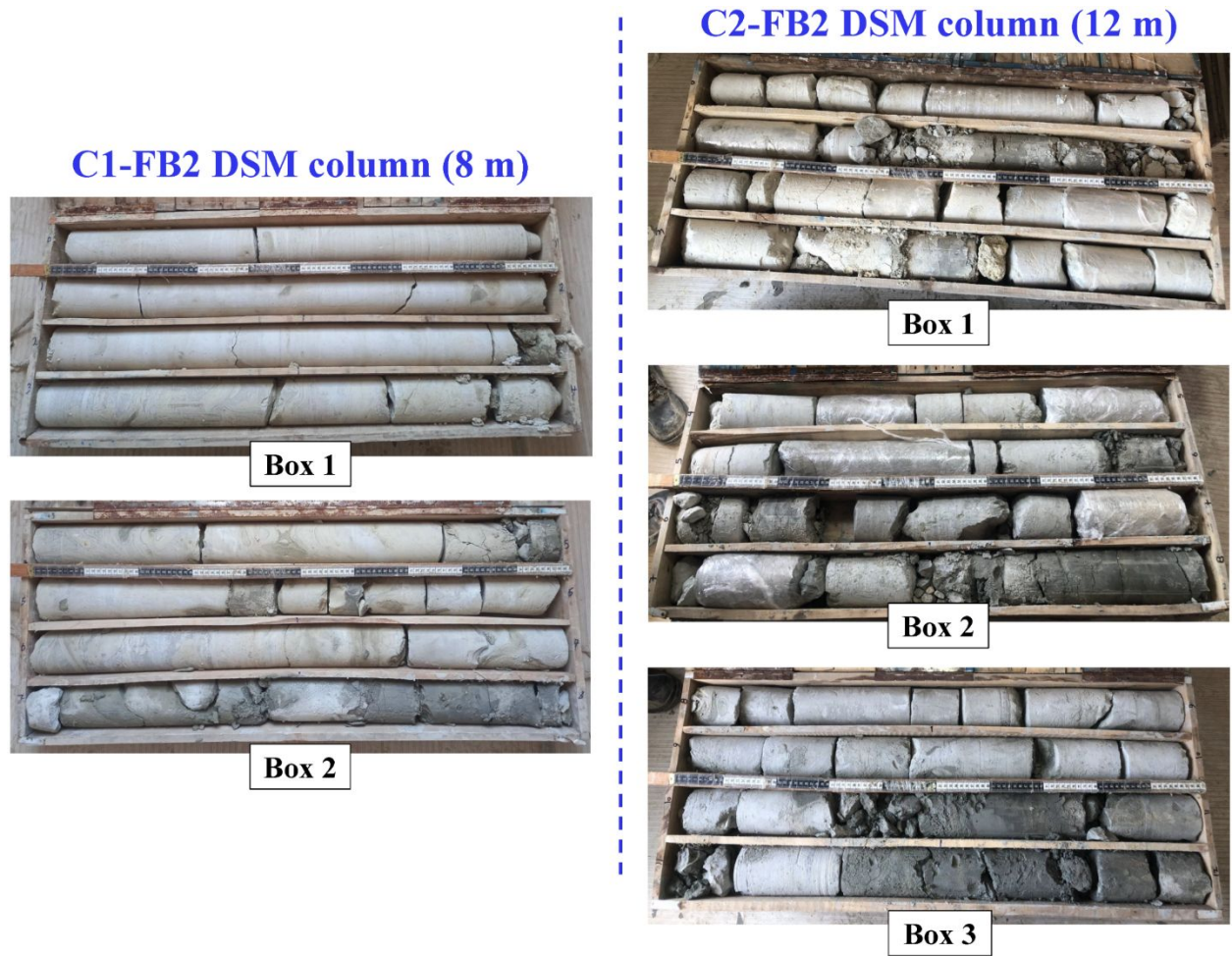


Fig. 15. Core box condition of DSM columns executed with auger FB-2 (with two free blade layers)

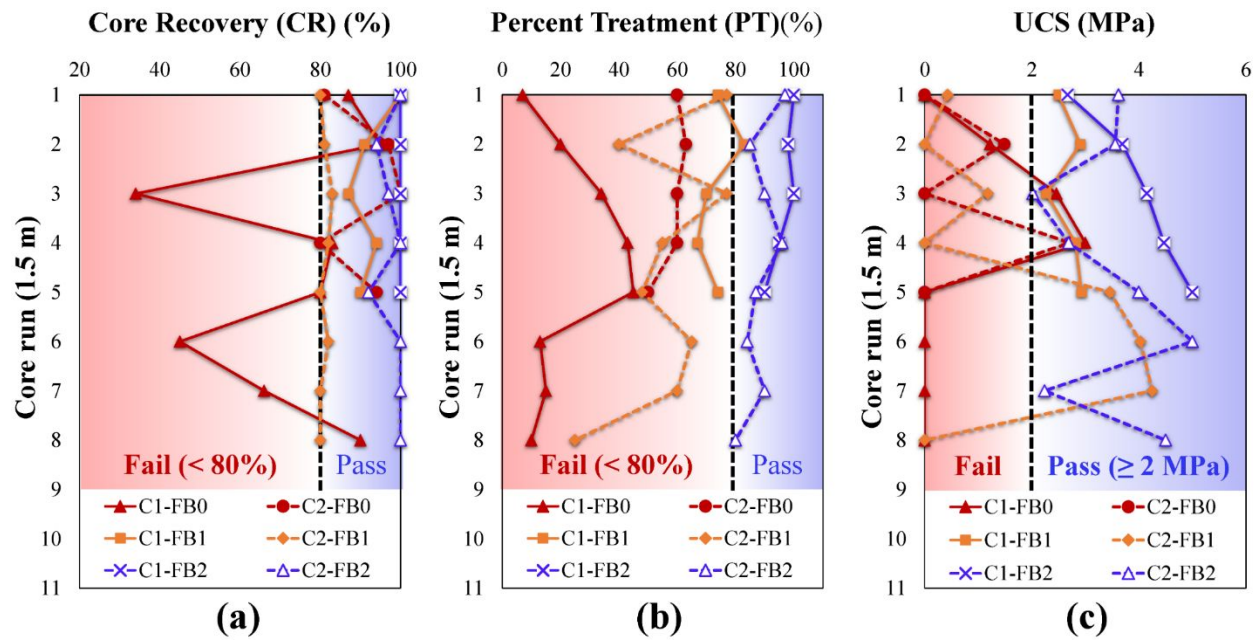


Fig. 16. Characteristics of example DSM columns executed with various augers: a) uniformity criterion (core recovery), b) uniformity criterion (percent treatment), and c) strength criterion (UCS test results)

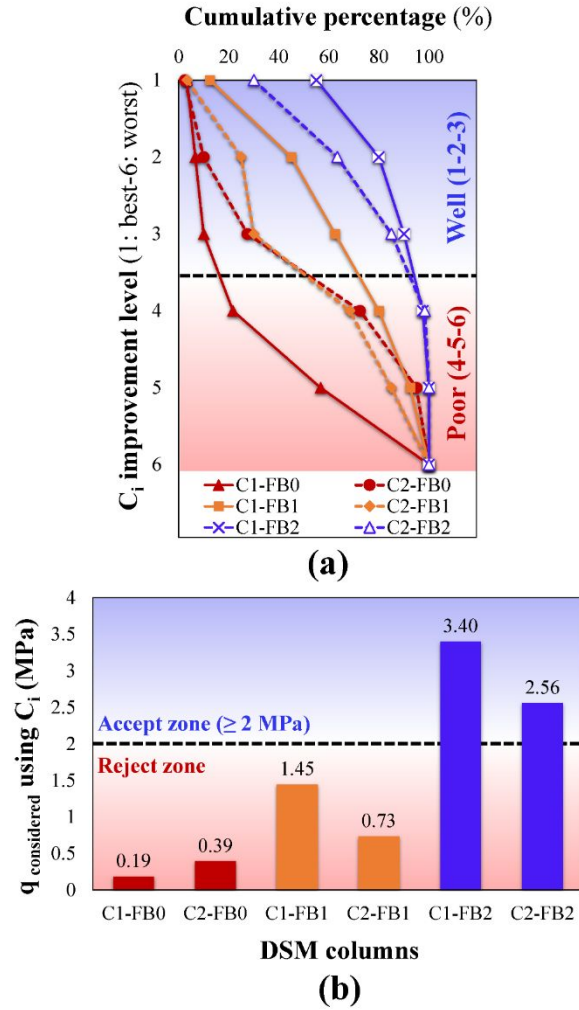


Fig. 17. a) Improvement levels of example DSM columns executed with various augers based on C_i evaluation method, and b) DSM column's representative strength based on C_i method

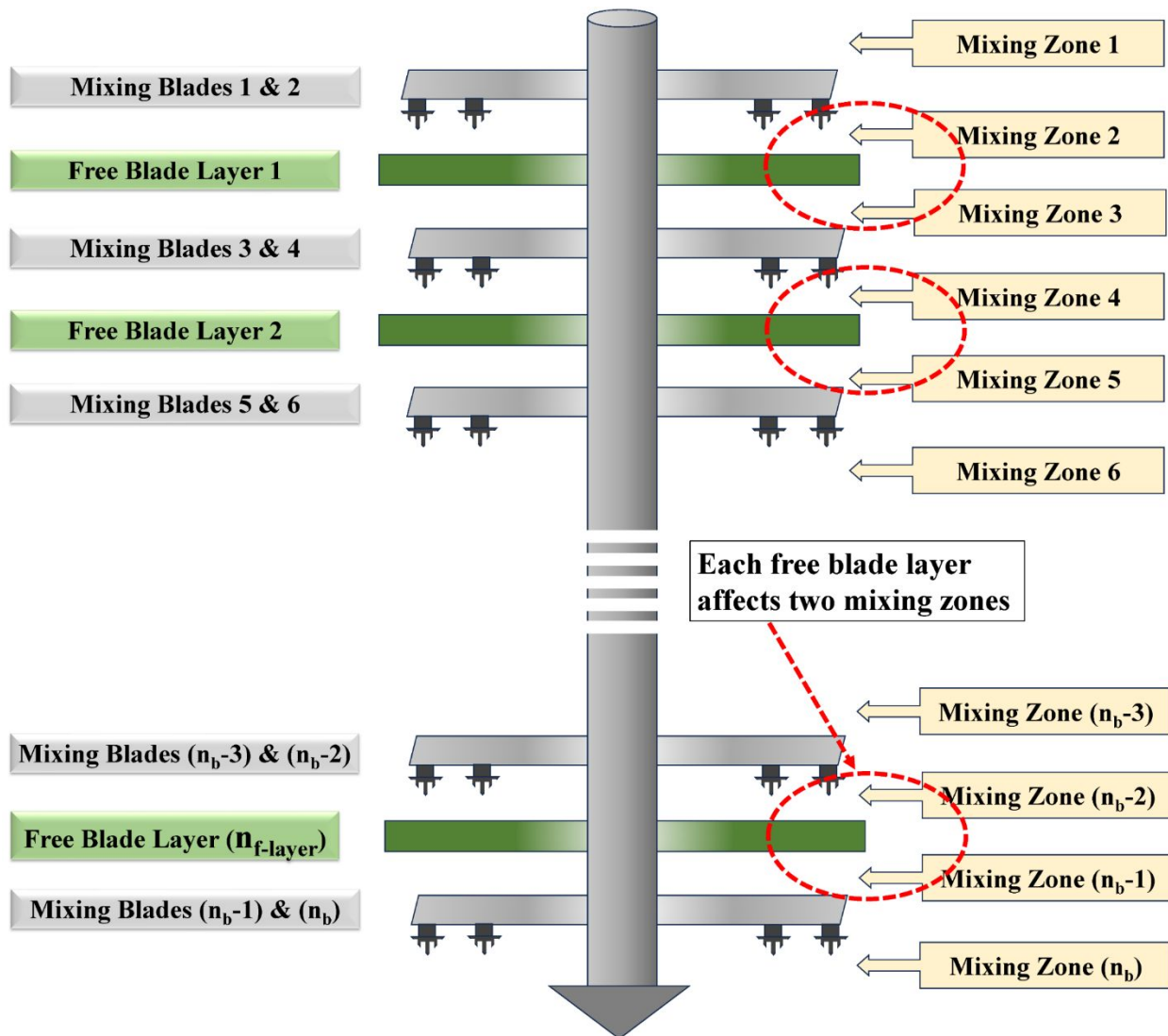


Fig. 18. Configuration of Mixing/Free blades and mixing zones in any desired auger with various blades

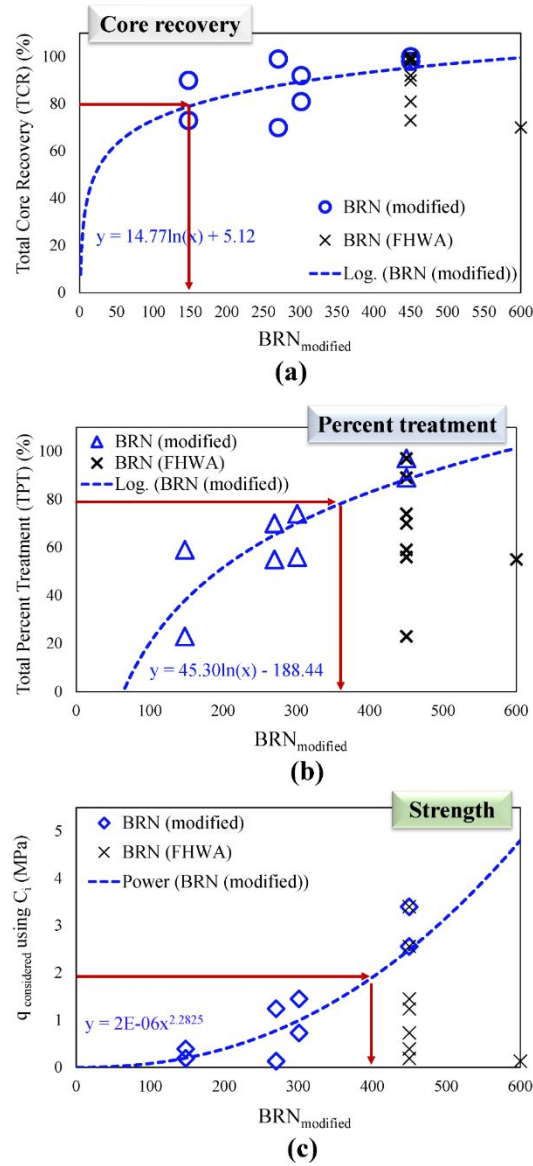


Fig. 19. Correlations between $BRN_{modified}$ parameter and quality indexes of DSM columns: a) core recovery, b) percent treatment, and c) representative strength based on C_i method